The Effect of Insulin on Glucose Metabolism

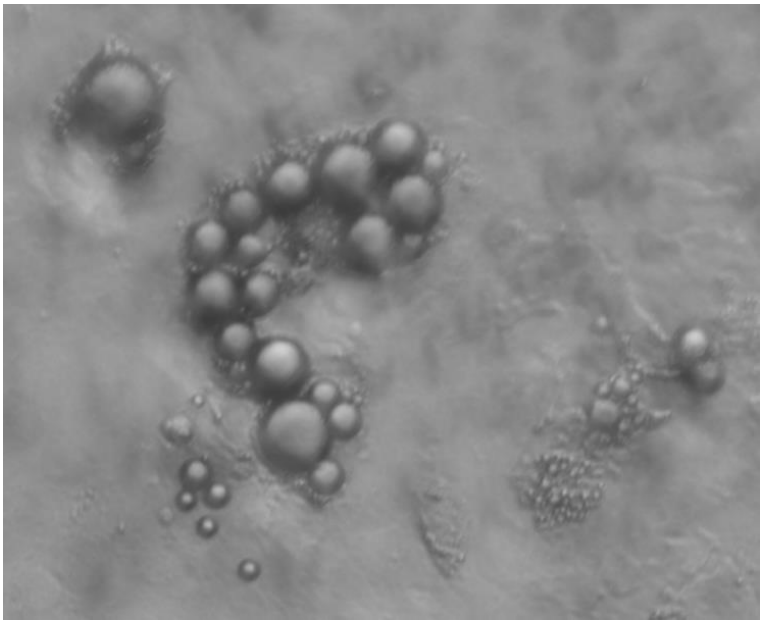

Eline Stoffers
Master Biomedical Sciences
First research project
Supervisors: Karen van Eunen & Barbara M. Bakker
24th of June 2015

CONTENTS

ABSTRACT

Development of T2DM is usually preceded by an increased metabolic demand for insulin due to insulin resistance in several tissues. We would like to elucidate the effect of insulin on glucose metabolism under insulin sensitive and resistant conditions, using TNF-α to induce insulin resistance in differentiated 3T3L1 cells.

As a pilot study first *in vitro* and *in vivo* NAD(P)H-linked enzyme assays were set up for the glycolytic enzymes. Overall the activity of the enzymes measured under *in vitro* conditions was slightly higher.

Using 2.5 nM TNF-α and 100 nM insulin, four cell conditions were made: without TNF-α without insulin, without TNF-α with insulin, with TNF-α without insulin and with TNF-α with insulin. In the four conditions differences in glucose-consumption, lactate-production, pyruvate concentration and glycolytic enzymes activities were determined. Glucose consumption was measured over 24 hours. TNF-α did not induce insulin resistance. However, it did decrease glucose consumption of cells. Insulin did increase glucose consumption. Lactate and pyruvate were measured in the medium at the 24 hour time point. Lactate production was increased by insulin and TNF-α, but no effects were seen on pyruvate concentration. The in vitro assays were used to measure enzyme activities. Insulin increased the activity of the enzymes, TNF-α had no effect on activity.

To conclude, no insulin resistance was induced. However, TNF-α still had an effect on the glucose metabolism. It caused decreased glucose consumption and more glucose to be converted to lactate. The mechanism behind this is unknown. A remarkable effect of insulin was the increased enzyme activities. A lot of research still has to be done to optimize the conditions of the experiment. In the future, in vivo conditions should be used and with these results a quantitative computer model of the glucose metabolism can be developed.

INTRODUCTION

Diabetes

The prevalence of diabetes is increasing worldwide and is a significant problem that needs to be addressed. Diabetes is a group of metabolic diseases characterized by hyperglycemia. Hyperglycemia is an increased blood glucose concentration and is the result of defects in insulin secretion, insulin action or both (American Diabetes Association, 2014). There are various types of diabetes, however this report will focus on type 2 diabetes mellitus (T2DM) (Al-Goblan et al., 2014; Karalliedde et al., 2014). Around 90% of the individuals with diabetes have T2DM (WHO, 2015). It is one of the most serious public health problems worldwide and is still increasing in prevalence (Feng et al., 2012). Currently, T2DM affects over 371 million people worldwide (Lai et al., 2014). Figure 1 shows that the prevalence is highest in North America and Caribbean, with a prevalence of 11.4% (International Diabetes Federation, 2014). Historically T2DM has been a disease mostly present in older adults, however it is nowadays also increasingly present in young adults and children. The increase in presence of T2DM in the younger population is due to increasing rates of obesity in the younger population (Karalliedde et al., 2014). Both genetic and environmental factors contribute to the development of T2DM. The environmental factors that promote T2DM are particularly high-caloric diets and a sedentary lifestyle, which also often lead to obesity (Al-Goblan et al., 2014; Goldstein et al., 2002; Lai et al., 2014; WHO, 2015).

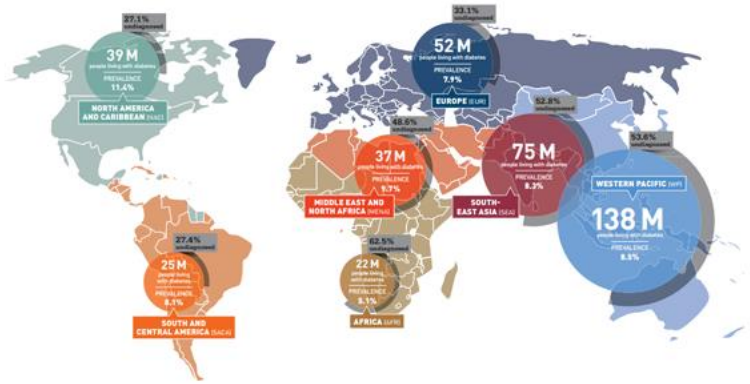

Figure 1. Worldwide distribution of diabetes (International Diabetes Federation, 2014).

Development of diabetes

Development of T2DM is usually preceded by an increased metabolic demand for insulin due to insulin resistance in several tissues (Kasuga et al., 2006; Al-Goblan et al., 2014). Insulin resistance causes a reduced sensitivity to insulin action in peripheral target tissues. Peripheral target tissues include skeletal muscle, adipose and liver tissues (Capursoa et al., 2014; Feng et al., 2012; Goldstein et al., 2002). Figure 2 shows the insulin actions when no insulin resistance is present.

In order to develop T2DM, insulin resistance and pancreatic β-cell dysfunction have to exist simultaneously (Al-Goblan et al., 2014). In the pre-stage of T2DM, when only insulin resistance is present, blood glycaemia levels are near normal. In this stage pancreatic β-cells compensate for the insulin resistance by hyper secretion of insulin. However, in the long run the β-cells will fail to compensate, the pancreas secretes insufficient insulin and diabetes arises (figure 3) (Kasuga et al., 2006; Al-Goblan et al., 2014).

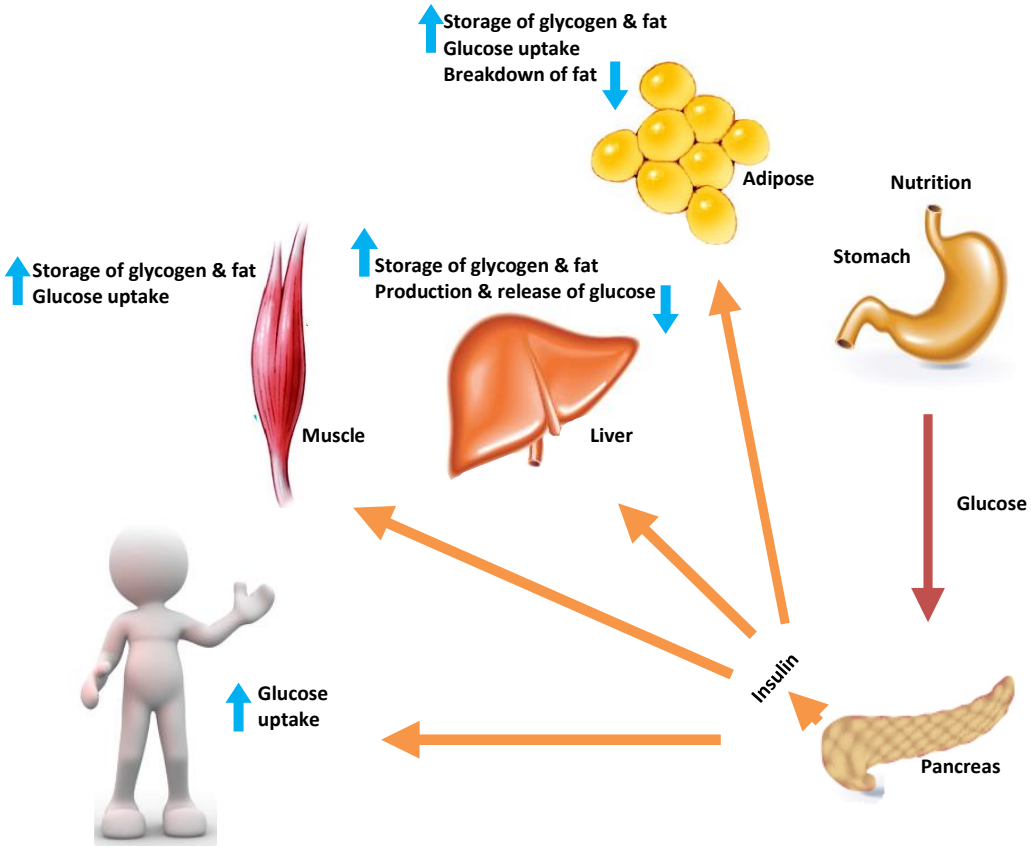

Figure 2. Insulin response to an increased glucose concentration in the blood. The pancreas senses an increased concentration of glucose in the blood and secretes insulin in response. Insulin increases glucose uptake in the body and storage of glycogen and fat and it decreases production and release of glucose by the liver and breakdown of fat in the adipose tissue (Goldstein et al., 2002; Kasuga et al., 2006).

Insulin resistance

Insulin resistance in the body affects many tissue functions and a variety of metabolic processes. There are various proposed mechanisms by which insulin resistance can be caused:

Tumor necrosis factor-a

Tumor necrosis factor-α (TNF-α) is an inflammatory cytokine and is mainly expressed in adipose tissue and macrophages (Capursoa et al., 2014). TNF-α inhibits the activity of many components in the insulin-signaling cascade (Kim et al., 2015). For instance, TNF-α inhibits insulin-stimulated tyrosine phosphorylation of the insulin receptor (IR) and leads to inactivation of the insulin receptor substrate 1 (IRS-1). TNF-α inactivates the IRS-1 via two mechanisms; first a dephosphorylation of tyrosine and second a serine phosphorylation at the serine 312 residue. With its effects on the IR and the IRS-1, TNF-α causes a down regulation of translocation of the insulin-sensitive glucose transporter GLUT-4 to the cell surface (Capursoa et al., 2014; Hotamisligil, 2000). Normally the GLUT-4 is translocated from cellular vesicles to the cell surface; there it mediates glucose transport into the cell. The glucose transport into the cell is decreased by TNF-α (Capursoa et al., 2014).

Free fatty acids

Increased levels of circulating free fatty acids (FFAs) also play a role in development of insulin resistance (Boden, 2003). Obese individuals often have excess visceral adiposity, which contributes to a chronic increase in circulating FFAs (Lai et al., 2014). The increased amount of circulating FFAs can cause insulin resistance (Capursoa et al., 2014, Feng et al., 2012). Insulin resistance causes an increased lipolysis in adipocytes, which then leads to an even more increased amount of circulating FFAs (Goldstein et al., 2002).

The increased levels of FFAs cause increased FFA uptake by muscle, liver and adipose tissue. When the FFA flux exceeds the ability of the tissues to dispose them, intermediates of the fatty-acid

metabolism accumulate. The intermediates are diaglycerol, phosphatidic acid, lysophosphatidic acid and ceramide. FFAs themselves or their intermediates can cause insulin resistance by having a negative impact on the activation and signaling cascade of the insulin receptor pathway. Like TNF-α, FFAs cause a phosphorylation of the serine 312 residue of IRS-1, which causes an interruption of the IR/IRS interaction and this interrupts the insulin-signaling pathway (Capursoa et al. 2014).

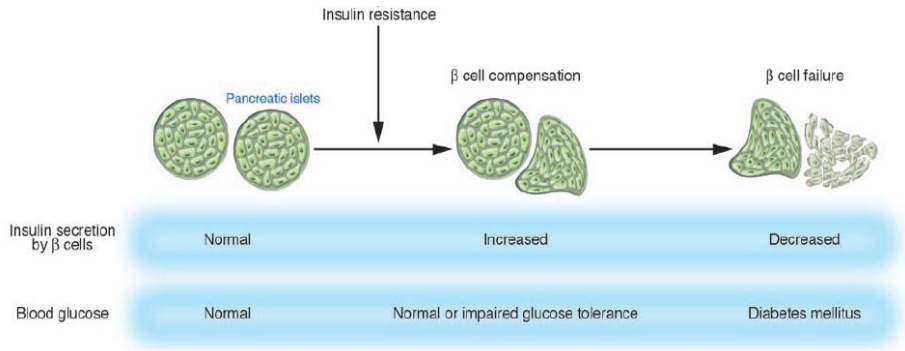

Figure 3. Development of type 2 diabetes mellitus. The development of T2DM is usually preceded by development of insulin resistance. At first the pancreatic β-cells compensate for insulin resistance by hyper secretion of insulin. However, at some point β-cell compensation is followed by β-cell failure and diabetes arises (Kasuga et al. 2006).

Outline

To obtain a better understanding of the mechanism underlying T2DM we investigated the effects of insulin on glucose metabolism. This resulted in the following research question: what is the effect of insulin on glucose metabolism under insulin sensitive and resistant conditions?

We will study the effect of insulin on glucose metabolism in a 3T3L1 pre-adipocyte fibroblast cell line, which will be differentiated to adipocytes. Adipocytes are used because they are one of the most highly insulin-responsive cell types. In adipocytes, insulin promotes glucose uptake and storage of glycogen and fat and it inhibits breakdown of fat, as shown in figure 2 (Kahn & Flier., 2000). In order to elucidate the effects of insulin on glucose metabolism we examined cells under two conditions, insulin sensitive and insulin resistant conditions. We induced insulin resistance using TNF-α. Previous research already showed that TNF-α has an effect on glucose transport. Insulin-dependent glucose transport is reduced when cells are incubated with TNF-α and insulin sensitivity is decreased, as shown in figure 4 (Lo et al., 2013). However, it has not yet been shown what the effect of TNF-α induced insulin resistance is on the rest of glucose metabolism. Here we will try to elucidate the effect of TNF-α-induced insulin resistance on the glucose-consumption and lactate-production rates, the pyruvate concentration and the activity of the glycolytic enzymes.

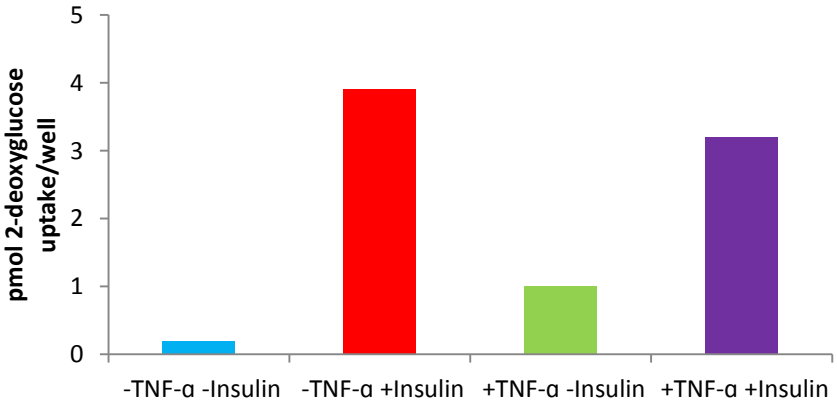

Figure 4. Insulin resistance by TNF-α. Glucose uptake in four conditions. Blue: without TNF-α without insulin, Red: without TNF-α with insulin, Green: with TNF-α without insulin and Purple: with TNF-α with insulin (Lo et al, 2013).

MATERIALS AND METHODS

Materials

Chemicals used were purchased from Sigma-Aldrich, Roche Applied Sciences and Santa Cruz Biotechnology. Culturing media were purchased from Gibco. Used equipment were a Synergy H4 Hybrid Multi-Mode Microplate plate reader from Biotek, a Vibra-cell sonicator from Sonics and a cell counter from Biorad.

Cells

Culturing

C2C12 cells and 3T3L1 cells were used for the experiments and cultured in Dulbecco's Modified Eagle Medium (DMEM) with 25 mM glucose 10 % Fetal Calf Serum (FCS) and 1 % Penicillin-Streptomycin (PS). Cells were cultured in a 37 ^{0}C stove with an atmosphere of 5 % CO_2. For passing the cells, medium was discarded; cells were rinsed two times with 5mL Hanks' Balanced Salt Solution (HBSS) and detached with 1 mL trypsin. Cells were passed at 70 % confluence.

Differentiation

3T3L1 cells were plated out in 6-wells plates with a cell density of 1.0-1.5*10^5 cells/mL. Differentiation started 48 hours after the cells reached confluence. For differentiation we used DMEM medium with 25 mM glucose, 10% Hyclone Fetal Bovine Serum, 1% PS, 960 nM insulin, 0.5 M 3-isobutyl-1-methylxanthine, 1 µM dexamethasone (in EtOH) and 2 µM rosiglitazone. After 48 hours the medium was changed to differentiation medium enriched with only 960 nM insulin (without the 3-isobutyl-1-methylxanthine, dexamethasone and rosiglitazone). Again 48 hours later the medium was changed to merely standard DMEM medium with FCS and PS. From the fifth day on medium was changed every other day to normal culturing medium. Differentiation was finished after two to three weeks when 70-80% differentiation into adipocytes was reached.

Enzyme activity assays

Activity assays of the glycolytic enzymes were done NAD(P)H-linked with freshly prepared cell extracts of undifferentiated C2C12 cells and differentiated 3T3L1 cells at 37 ^{0}C in a 96-wells plate. Samples were taken from the -80 ^{0}C and thawed on ice. 1 mM dithiothreitol (DTT) was added and samples were sonicated for 30 seconds with a pulse every other second and an amplitude of 20 %. Two, four and eight times dilutions of the cell extract were made using 0.01 M potassium phosphate buffer pH 7.0 with 1 mM DTT. Pre-warmed (37 ^{0}C) assay mixture was added to the four dilutions of the cell extracts and the water (control). The assay mixture contained the *in vitro* or *in vivo* medium mentioned in the sections below.

First a baseline measurement was done containing sample and assay mixture. Then 25 µL of a start reagent was added and the production or consumption of NAD(P)H was measured at 340 nM in a plate reader. The slope of the NAD(P)H production or consumption represented the activity of the enzyme. The activity of the enzymes was expressed in µmol per minute per mg protein.

Enzyme activity was normalized for protein concentration of the cell extracts. Protein concentration in the extract was measured with a Bicinchoninic Acid kit (BCA Protein assay kit; Pierce) with Bovine Serum Albumin (BSA) (2 mg/mL stock solution; Pierce) containing 1 mM DTT as standard. A standard curve was made in a range of 0 to 1.2 mg/mL BSA in 0.01 M potassium phosphate buffer pH 7.0 with 1 mM DTT. 10 µL of each BSA standard was added in duplo to a 96 well plate. 10 µL of the undiluted and the two, four and eight times diluted cell extracts were also added in triplo. 200 µL of the BCA reagent of the BCA Protein Assay Kit was added to the wells and the plate was incubated at 37 ^{0}C for 30 minutes. Afterwards absorbance was measured using a plate reader at 562 nanometer.

In vitro assays

Hexokinase (HXK) converts glucose to glucose-6-phosphate. The following reaction was used to measure the activity of the HXK enzyme:

Glucose + ATP $\xrightarrow[\text{HXK}]{}$ ADP + Glucose-6-phosphate

Glucose-6-phosphate + $NADP^+$ $\xrightarrow[\text{G6PDH}]{}$ 6-Phosphogluconolactone + NADPH

The buffer of the assay mixture contained 0.5 M imidazole (pH 7.6) and 0.5 M magnesium chloride ($MgCl_2$). 0.1 M glucose was used as a substrate and 0.04 M NADP was used as a cofactor. The coupling enzyme used in this reaction was 1750 U/mL glucose-6-phosphate dehydrogenase (G6PDH). This mixture was added to 25 µL of cell extract. The reaction was started with 0.01 M ATP.

Phosphoglucose-isomerase (PGI) converts fructose-6-phosphate to glucose-6-phosphate. The following reaction was used to measure the activity of the PGI enzyme:

Fructose-6-phosphate $\xrightarrow[\text{PGI}]{}$ Glucose-6-phosphate

Glucose-6-phosphate + $NADP^+$ $\xrightarrow[\text{G6PDH}]{}$ 6-Phosphogluconolactone + NADPH

The buffer of the assay mixture contained 1 M Tris-HCl (pH 8.0) and 0.5 M $MgCl_2$. 0.04 M NADP was used as a cofactor. The coupling enzyme used in this reaction was 1750 U/mL G6PDH. This mixture was added to 5 µL of cell extract. The reaction was started with 0.02 M fructose-6-phosphate.

Glucose-6-phosphate dehydrogenase converts glucose-6-phosphate to 6-phosphogluconolactone. The following reaction was used to measure the activity of the G6PDH enzyme:

Glucose-6-phosphate + $NADP^+$ $\xrightarrow[\text{G6PDH}]{}$ 6-Phosphogluconolactone + NADPH

The buffer of the assay mixture contained 1 M Tris-HCl (pH 8.0) and 0.5 M $MgCl_2$. 0.04 M NADP was used as a cofactor. This mixture was added to 25 µL of cell extract. The reaction was started with 0.05 M glucose-6-phosphate.

Phosphofructokinase (PFK) converts fructose-6-phosphate to glucose-6-phosphate. The following reaction was used to measure the activity of the PFK enzyme:

Fructose-6-phosphate + ATP $\xrightarrow[\text{PFK}]{}$ Fructose-1,6-bisphosphate + ADP

Fructose-1,6-bisphosphate $\xrightarrow[\text{ALD}]{}$ DHAP + Glyceraldehyde-3-phosphate

DHAP $\xrightarrow[\text{TPI}]{}$ Glyceraldehyde-3-phosphate

2 DHAP + 2 NADH $\xrightarrow[\text{G3PDH}]{}$ 2-Glycerol-3-phosphate + 2 NAD^+

The buffer of the assay mixture contained 1 M Tris-HCl (pH 8.0), 0.5 M $MgCl_2$ and 1 M potassium chloride (KCl). 0.015 M NADH and 0.1 M ATP were used as cofactors. The coupling enzymes used in this reaction were 90 U/mL fructose-1,6-bisphosphate aldolase, 620 U/mL glycerol-3-phosphate dehydrogenase and 1800 U/mL triose phosphate isomerase. This mixture was added to 25 µL of cell extract. The reaction was started with 0.02 M fructose-6-phosphate.

Fructose-1,6-bisphosphate aldolase (ALD) converts fructose 1,6-bisphosphate to glyceraldehyde-3-phosphate. The following reaction was used to measure the activity of the ALD enzyme:

Fructose-1,6-bisphosphate $\xleftrightarrow[\text{ALD}]{}$ Glyceraldehyde-3-phosphate + DHAP

Glyceraldehyde-3-phosphate $\xleftrightarrow[\text{TPI}]{}$ DHAP

2 DHAP + 2 NADH $\xleftrightarrow[\text{G3PDH}]{}$ 2-Glycerol-3-phosphate + 2 NAD^+

The buffer of the assay mixture contained 1M Tris-HCl (pH 7.5) and 1 M KCl. 0.015 M NADH was used as a cofactor. The coupling enzymes used in this reaction were 620 U/mL glycerol-3-phosphate dehydrogenase and 1800 U/mL triose phosphate isomerase. This mixture was added to 5 µL of cell extract. The reaction was started with 0.02 M fructose-1,6-bisphosphate.

Triose phosphate isomerase (TPI) converts glyceraldehyde-3-phosphate to DHAP. The following reaction was used to measure the activity of the TPI enzyme:

Glyceraldehyde-3-phosphate $\xleftrightarrow[\text{TPI}]{}$ DHAP

2 DHAP + 2 NADH $\xleftrightarrow[\text{G3PDH}]{}$ 2-Glycerol-3-phosphate + 2 NAD^+

The buffer of the assay mixture contained 1M triethanolamine-HCl (pH 8.2). 0.015 M NADH was used as a cofactor. The coupling enzyme used in this reaction was 1700 U/mL glycerol-3-phosphate-dehydrogenase. This mixture was added to 5 µL of cell extract. The reaction was started with 0.058 M glyceraldehyde-3-phosphate.

Glyceraldehyde-3-phosphate dehydrogenase (GAPDH) converts 3-phosphate-glycerate to 1,3-diphosphoglycerate. The following reaction was used to measure the activity of the GAPDH enzyme:

3-phosphate-glycerate + ATP $\xleftrightarrow[\text{GAPDH}]{}$ 1,3-diphosphoglycerate + ADP

1,3-diphosphoglycerate + NADH $\xleftrightarrow[\text{PGK}]{}$ Glyceraldehyde-3-phosphate + NAD^+

The buffer of the assay mixture contained 1 M triethanolamine-HCl (pH 7.6), 0.02 M EDTA and 0.1 M $MgSO_4$. 0.015 M NADH and 0.1 M ATP were used as cofactors. The coupling enzyme used in this reaction was 4500 U/mL 3-phosphoglycerate kinase. This mixture was added to 5 µL of cell extract. The reaction was started with 0.05 M 3-phosphoglyceric acid.

Phosphoglycerate kinase (PGK) converts 3-phospho-glycerol phosphate to glyceraldehyde-3-phosphate. The following reaction was used to measure the activity of the PGK enzyme:

3-phospho-glycerate + ATP $\xleftrightarrow[\text{GAPDH}]{}$ 3-phospho-glycerol phosphate + ADP

3-phospho-glycerol phosphate + NADH $\xleftrightarrow[\text{PGK}]{}$ Glyceraldehyde 3-phosphate + NAD^+

The buffer of the assay mixture contained 1 M triethanolamine-HCl (pH 7.6), 0.02 M EDTA and 0.1 M $MgSO_4$. 0.015 M NADH and 0.1 M ATP were used as cofactors. This mixture was added to 5 µL of cell extract. The reaction was started with 0.05 M 3-phosphoglyceric acid.

Phosphoglycerate mutase (PGM) converts 3-phospho-glycerate and 2,3-diphosphoglycerate to 2-phospho-glycerate and 2,3-diphosphoglycerate. The following reaction was used to measure the activity of the PGM enzyme:

3-phospho-glycerate + 2,3-diphosphoglycerate $\xleftrightarrow[\text{PGM}]{}$ 2-phospho-glycerate + 2,3-diphosphoglycerate

2-phospho-glycerate $\xleftrightarrow[\text{ENO}]{}$ Phosphoenolpyruvate

Phosphoenolpyruvate + ADP $\xleftrightarrow[\text{PYK}]{}$ ATP + Pyruvate

Pyruvate + NADH $\xleftrightarrow[\text{LDH}]{}$ Lactate + NAD^+

The buffer of the assay mixture contained 1 M triethanolamine-HCl (pH 7.6) and 0.1 M $MgSO_4$. 0.015 M NADH, 0.1 M ADP and 0.125 M 2,3-diphospho-glyceric acid were used as cofactors. The coupling enzymes used in this reaction were 250 U/mL enolase, 2599 U/mL pyruvate kinase and 2859 U/mL lactate dehydrogenase. This mixture was added to 5 µL of cell extract. The reaction was started with 0.05 M 3-phosphoglyceric acid.

Enolase (ENO) converts 2-phospho-glycerate to phosphoenolpyruvate. The following reaction was used to measure the activity of the ENO enzyme:

2-Phosphoglyceric acid $\xleftrightarrow[\text{ENO}]{}$ Phosphoenolpyruvate

Phosphoenolpyruvate + ADP $\xleftrightarrow[\text{PYK}]{}$ ATP + Pyruvate

Pyruvate + NADH $\xleftrightarrow[\text{LDH}]{}$ Lactate + NAD^+

The buffer of the assay mixture contained 1 M triethanolamine-HCl (pH 8.0) and 0.1 M $MgSO_4$. 0.015 M NADH and 0.1 M ADP were used as cofactors. The coupling enzymes used in this reaction were 1813 U/mL pyruvate kinase and 2750 U/mL lactate dehydrogenase. This mixture was added to 25 µL of cell extract. The reaction was started with 0.01 M 2-phosphoglyceric acid.

Pyruvate kinase (PYK) converts phosphoenolpyruvate to pyruvate. The following reaction was used to measure the activity of the PYK enzyme:

Phosphoenolpyruvate + ADP $\xleftrightarrow[\text{PYK}]{}$ Pyruvate + ATP

Pyruvate + NADH $\xleftrightarrow[\text{LDH}]{}$ Lactate + NAD^+

The buffer of the assay mixture contained 0.5 M cacodylic acid (pH 6.2), 0.5 M $MgCl_2$ and 1 M KCl. 0.015 M NADH, 0.1 M ADP and 0.02 M fructose-1,6-biphosphate were used as cofactors. The coupling enzyme used in this reaction was 5000 U/mL lactate dehydrogenase. This mixture was added to 5 µL of cell extract. The reaction was started with 0.02 M phosphoenolpyruvate.

Lactate dehydrogenase (LDH) converts pyruvate to lactate. The following reaction was used to measure the activity of the LDH enzyme:

Pyruvate + NADH $\xleftrightarrow[\text{LDH}]{}$ Lactate + NAD^+

The buffer of the assay mixture contained 0.5 M hepes (pH 7.4), 0.5 M $MgCl_2$ and 1 M KCl. 0.015 M NADH was used as a cofactor. This mixture was added to 5 µL of cell extract. The reaction was started with 0.01 M pyruvate.

In vivo assays

In the enzyme assay with the vivo medium the same buffer was used for all the glycolytic enzymes.
The *in vivo* medium conditions that were used were a 1 M Tris-HCl buffer pH 7.0 (Barany, 1996; Bruch et al., 1976; Civelec et al., 1996; Groen et al., 1983; Ishibashi & Cottam, 1978; Oudard et al., 1996), a phosphate concentration of 5 mM (Conley et al., 1997; Guynn et al., 1973), a potassium concentration of 140 mM (Guynn et al., 1973; Østergaard, 1986; Rorsman & Trube, 1985; Tschopp & Schroder, 2010), a sodium concentration of 15 mM (Guynn et al., 1973; Lidofsky et al., 1993), a chloride concentration of 155 mM (Breitwieser et al., 1990; Janssen & Sims, 1992), a magnesium concentration of 0.5 mM (Guynn et al., 1973; Ingwall, 1982; Murphy et al., 1969), and a calcium concentration of 0.5 mM. In order to acquire these concentrations in the buffer of the assay mixture, a mixture of; 1 M of KCl, 150 mM of NaCl, 0.1 M of $MgSO_4$ and 0.5 mM $CaCl_2$ was used.
In addition to the buffer, the substrates, cofactors, coupling enzymes and start reagents necessary for the reaction to measure the activity were added as mentioned in the previous section. The same amount of sample was used in the *in vitro* and *in vivo* assays.

Glucose consumption experiment

The differentiated 3T3L1 cells were used for this experiment. The 6-wells plates were divided in four conditions; without TNF-α without Insulin, without TNF-α with Insulin, with TNF-α without Insulin and with TNF-α with Insulin.

Experimental procedure and sample collection

Medium was removed from the cells and cells were washed two times with 2 mL Phosphate-buffered saline (PBS). Afterwards cells were incubated with serum-free medium; DMEM with 5 mM glucose and 1 % PS for three hours. After three hours half of the cells were incubated with 2.5 nM TNF-α for 24 hours. After 24 hours cells were stimulated with 100 nM insulin for 30 minutes and also a control without insulin was included. After the incubation with insulin the experiment started. The medium

was removed from the cells and fresh medium was added. The medium contained serum-free DMEM with 1 % PS, 1 or 5 mM glucose and for half of the cells 100 nM insulin. Glucose concentration was dependent on the experiment; experiment 1 is with 1 and 5 mM and experiment 2 only with 5 mM of glucose. Insulin was added when the cells were incubated with insulin in the previous phase of the experiment. Every hour a 50 µL medium sample was taken of all the wells (experiment 1: t=0 - 4 hours and 24 hours; experiment 2: t=0 - 10 hours). At t=24h for the first experiment and t=10h for the second experiment a 200µL medium sample was taken and 20µL of 35% perchloric acid (PCA) was added to this sample. This sample with PCA was used for lactate and pyruvate measurements. The samples and remaining medium were stored in -80^{0}C. The cells were harvested at t=24h (first experiments) or t=10h (second experiment) as described in in the section below. In figure 5, an overview of the experiment is shown.

Harvesting of the cells

Medium was removed of the 6-wells plates and cells were washed with PBS. Cells were detached from the wells using trypsin followed by scraping of the wells, cells were taken up in medium (DMEM, 10% FCS and 1% PS) and transferred to tubes. Tubes were centrifuged at 94 rcf at 4 ^{0}C and supernatant was discarded. Pellets were resuspended in 300 µL 100 mM phosphate buffer pH 7, and stored in -80 ^{0}C.

Glucose concentration determination

Glucose concentration in the medium samples was enzymatically determined by measuring the amount of NADPH produced according to the following reactions:

$$\text{Glucose} + \text{ATP} \xleftrightarrow[\text{HXK}]{} \text{ADP} + \text{Glucose-6-phosphate}$$

$$\text{Glucose-6-phosphate} + \text{NADP}^+ \xleftrightarrow[\text{G6PDH}]{} \text{6-Phosphogluconolactone} + \text{NADPH}$$

First a standard curve was made with a range of 0.1 – 1 mM glucose, diluting 10 mM glucose in a 100 mM pipes buffer pH 7.0. The 5 mM glucose samples were 10 times diluted with 100 mM pipes buffer to fit within the standard curve. 25 µL of the standards and glucose samples were added in duplo to a 96-wells plate. 55 µL demi water was added to the wells. Afterwards 125 µL of a solution of 3 mL 100 mM pipes buffer, 150 µL 40 mM NADP, 120 µL 100 mM ATP, 60 µL 0.5 M $MgSO_4$ and 2 mL demi water was added to each well. After that 10 µL of a solution of 480 µL 100 mM pipes buffer, 10 µL 1389 U/mL hexokinase and 10 µL 1750 U/mL glucose-6-phosphate dehydrogenase was added to each well. This started the reaction. The NADPH absorbance was measured at 340 nm in a plate reader, when the reaction was finished after about 45 minutes.

Lactate and pyruvate concentration

Samples collected during the glucose consumption experiment of 200 µL culture medium with 20 µL 35 % PCA solution were taken from the -80 ^{0}C freezer and thawed on ice. All samples were vortexed two times. 150 µL of the sample was transferred into a fresh tube. The sample was neutralized with 15 µL 5 M KOH in 0.2 M MOPS and vortexed once more. Afterwards samples were centrifuged for 5 minutes at 21130 rcf at 4 ^{0}C. The supernatant was transferred to a fresh tube and lactate and pyruvate concentrations were measured in the solution.

To measure lactate concentrations the increase of absorbance of NADH was measured using the following reaction:

$$\text{Lactate} + \text{NAD}^+ \xrightarrow[\text{LDH}]{} \text{Pyruvate} + \text{NADH}$$

With pyruvate the decrease in NADH absorbance was measured according to the following reaction:

Pyruvate + NADH $\xrightarrow[\text{LDH}]{}$ Lactate + NAD^+

With the changes in NADH absorbance at 340 nm the concentration of lactate and pyruvate were calculated (Bergmeyer, 1970).

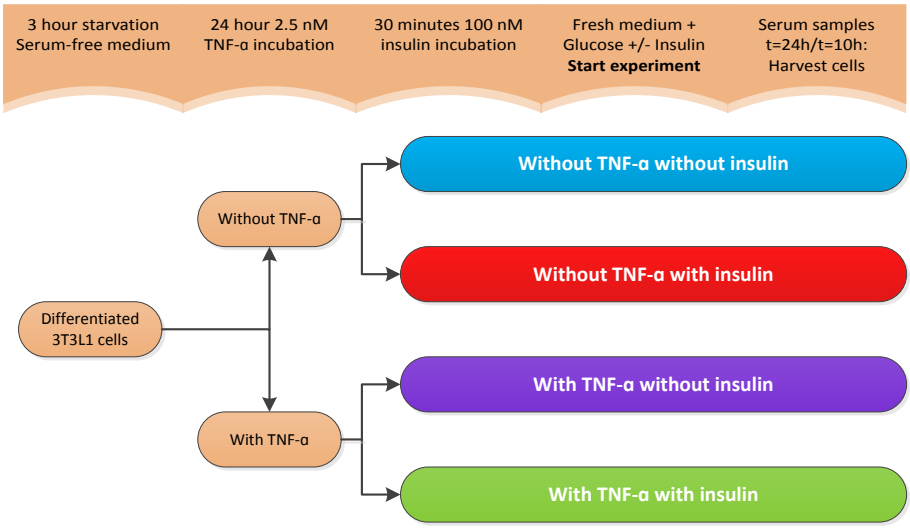

Figure 5. Schematic overview of the insulin-resistance experiment with differentiated 3T3L1 cells.

Statistical analysis

A Two-Way ANOVA with a Bonferroni post-test was used for statistical analysis. Differences were significant when $p > 0.05$ (*), $p > 0.01$ (**) or $p > 0.001$ (***). Data was analysed using Excel 2010 and GraphPad Prism 5.00.

RESULTS

In this study we have tried to elucidate the mechanism behind the development of insulin resistance in adipocytes. We expected that in insulin-resistant cells, the glucose consumption, lactate production and the activity of the glycolytic enzymes would be decreased. Because when insulin resistance is present glucose uptake is decreased, and for that reason probably also the metabolism of glucose. Figure 6 gives an overview of the project.

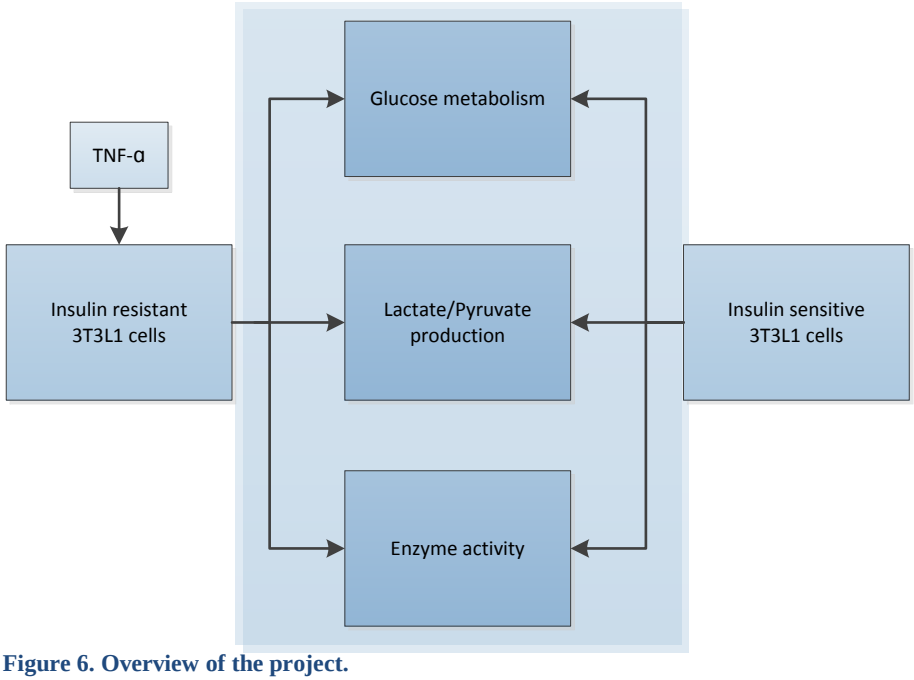

Figure 6. Overview of the project.

Set up of the enzyme assays

Assays for the glycolytic enzymes under in vitro and in vivo conditions functioned properly

Assays to determine the activity of the glycolytic enzymes were successfully set up and activity was measured for all enzymes in C2C12 cells. This study was a pilot study to measure enzyme activity under different conditions. Enzyme assays were performed under two conditions, *in vitro* and *in vivo* conditions. *In vitro* conditions are conditions optimized for each enzyme to get the highest activity. *In vivo* conditions are conditions that closely resemble the cytosol. Enzyme assays were done under *in vivo* conditions, because the results of the *in vivo* conditions are necessary for a quantitative computer model. Figure 7 shows the activities of the glycolytic enzymes under the two conditions. HXK, G6PDH, PFK, ALD and ENO were enzymes low in activity and PGI, GAPDH, PGK, PYK, LDH and TPI were enzymes higher in activity. Overall the activity of the enzymes measured using the *in vitro* conditions were slightly higher than when *in vivo* conditions were used. This is what was expected, because the *in vitro* conditions are optimized for each enzyme to get the highest activities possible.

The enzyme assays were done using cell extracts in different dilutions. With the results of the dilutions enzyme activities were calculated. To check whether the measured enzyme was the only limiting factor we checked the proportionality in which we compared the enzyme activity with the fraction of the sample present. When the enzyme is the only limiting factor, the enzyme activity and fraction of sample would be proportional. In our experiments the proportionalities were between 0.92 and 1, so the measured enzyme is the only limiting factor. The results of the proportionality check can be found in supplement 1 figure 1.

To conclude, the enzyme assays are functioning properly and can be used for the following experiments. The *in vitro* enzyme assays will be used for the following experiments, since they give

higher activity and therefore easier to measure in the small amount of cells available from the experiment. However, later we need the results of the *in vivo* conditions for a quantitative computer model.

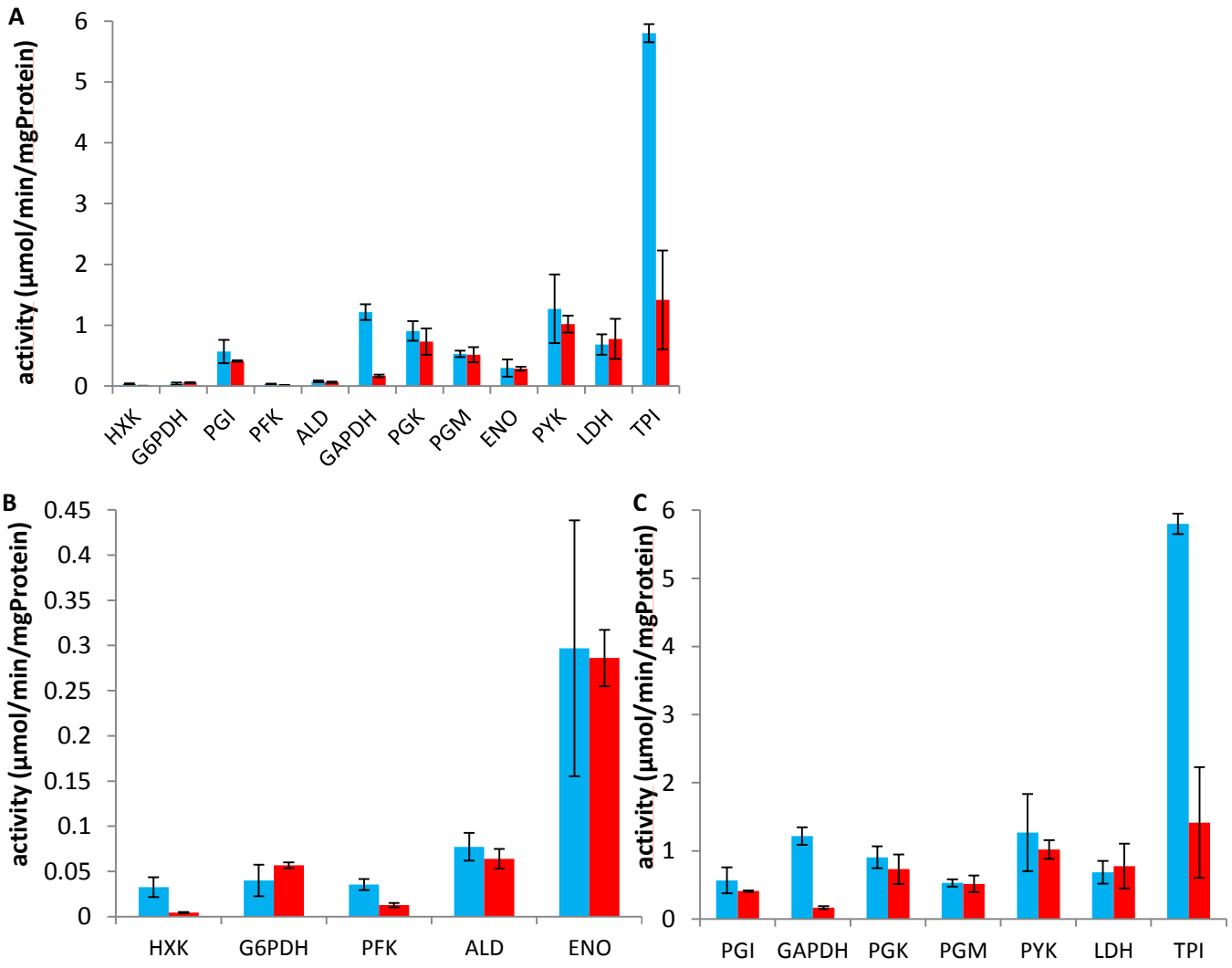

Figure 7. Activity of the glycolytic enzymes under *in vitro* and *in vivo* conditions. A) An overview of all enzymes. B) Enzymes with lower activity. C) Enzymes with higher activity. Blue: *In vitro* conditions, Red: *In vivo* conditions. Error bars represent the standard deviation.

Cells

3T3L1 cells were differentiated to adipocytes with different success rates

The 3T3L1 cells had to be differentiated from fibroblasts to adipocytes. In the first experiment differentiation functioned properly, 70-80 % of the cells were differentiated after three weeks. However, in the second experiment differentiation did not go as good, only 20- 40 % of the cells were differentiated. In figure 8 a picture of an adipocyte is shown.

Inducing insulin resistance in adipocytes

The main goal of this experiment was to optimize the conditions to induce insulin resistance in adipocytes. The first set of 3T3L1 cells with 70-80% differentiated cells was used for this experiment. 3T3L1 cells were first treated with TNF-α and insulin to get the four cell conditions: without TNF-α without insulin, without TNF-α with insulin, with TNF-α without insulin and with TNF-α with insulin. Furthermore, two glucose concentrations were used in this experiment, 1 mM and 5 mM of glucose (figure 9-12).

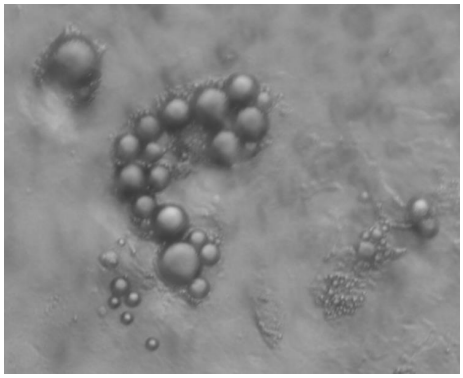

Figure 8. A differentiated adipocyte. Picture was made by bright field microscopy, Zen 2012 (blue edition) with a 100x magnification.

An optimal time frame to determine glucose consumption rate still has to be found

To figure out the optimal time frame to measure to glucose consumption rate of the cells, we started with a time frame of 24 hours. Medium samples were taken for the first four hours and one after 24 hours. With both concentrations of glucose there were no detectable changes in glucose concentrations in the first four hours of the experiment. However, at the time point of 24 hours there were detectable changes in glucose concentration in the medium (figure 9). So, the changes took place in the last 20 hours in which no additional measurements were done. Another experiment should be done in which samples are also taken in the last 20 hours to determine the optimal time frame of the experiment.

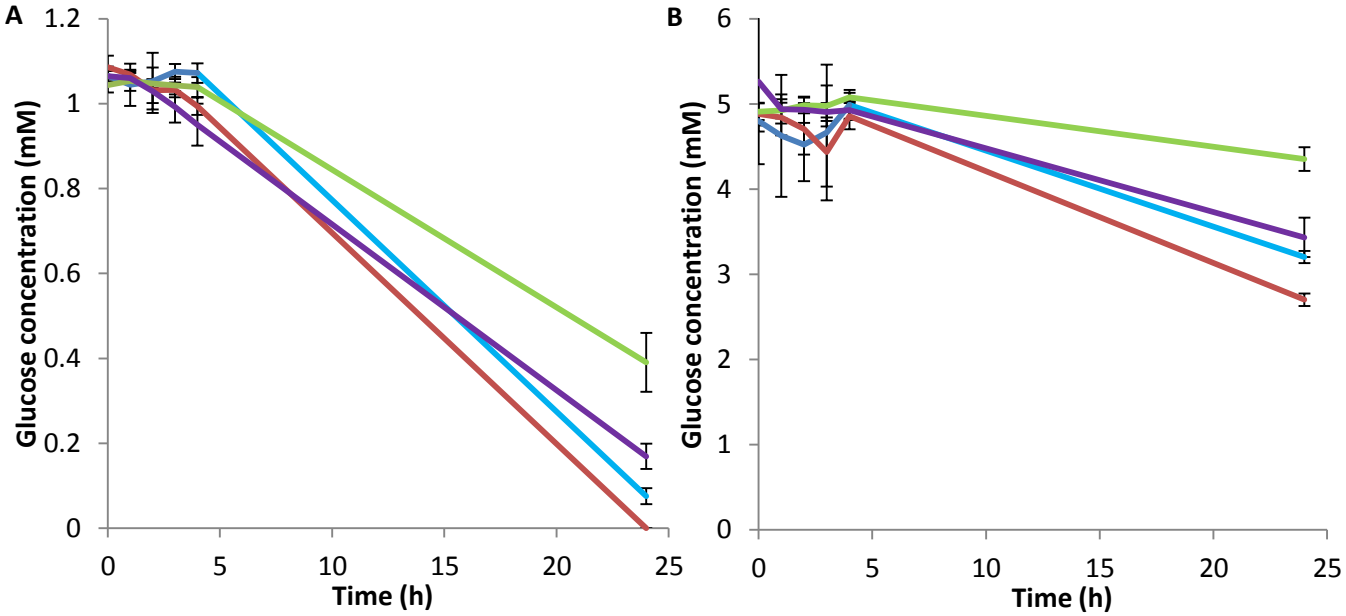

Figure 9. Effect of TNF-α and insulin on glucose consumption in a time frame of 24 hours at glucose concentrations of 1 and 5 mM of glucose. A) 1 mM glucose concentration. B) 5 mM glucose concentration. Blue: without TNF-α without insulin, Red: without TNF-α with insulin, Green: with TNF-α without insulin and Purple: with TNF-α with insulin.

5 mM of glucose seemed the best glucose concentration to determine glucose consumption rate

To determine what glucose concentration was best to determine glucose consumption rate, we used 1 and 5 mM of glucose. In both concentrations a change in glucose concentration in the medium was detected after 24 hours (figure 9). However, when 1 mM of glucose was used, the glucose was finished before the end of the experiment for one condition. Therefore, we could not use these results further. When 5 mM of glucose was used, there still was glucose left in all four conditions, so these results could be used. Another advantage of using 5 mM of glucose is that this is the physiological concentration (Kleman et al., 2009). For these reasons 5 mM of glucose seemed to be the best glucose concentration to use to determine the glucose consumption rate of the cells. The rest of the results will be based on the experiment with 5 mM glucose.

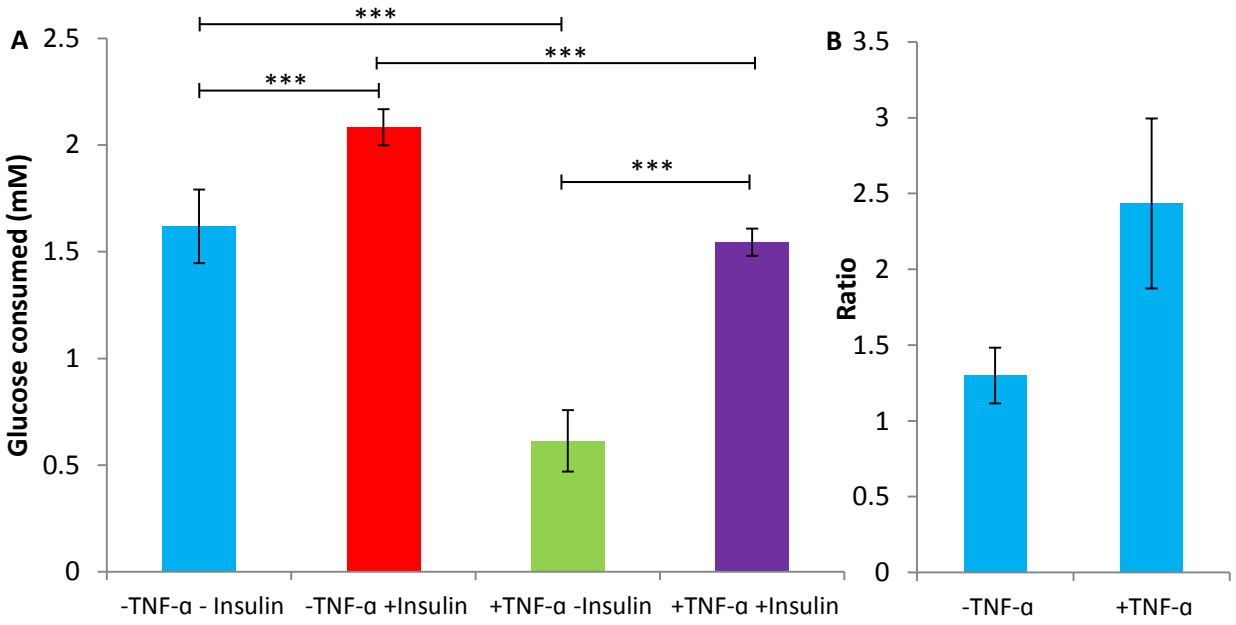

Figure 10. Effect of TNF-α and insulin on glucose consumption and insulin sensitivity in a time frame of 24 hours. A) Glucose consumption. B) Insulin sensitivity ratios of the conditions without and with TNF-α (Statistics could not be applied since we had not enough samples). Blue: without TNF-α without insulin, Red: without TNF-α with insulin, Green: with TNF-α without insulin and Purple: with TNF-α with insulin. Error bars represent standard deviation. * = $p < 0.05$ ** = $p < 0.01$ *** = $p < 0.001$.

TNF-α did not induce insulin resistance, however it did decrease glucose consumption of cells

This experiment was performed to determine the differences in glucose consumption between the four conditions. With the differences between the glucose concentration in the medium at the start and end of the experiment (figure 9B), the amount of glucose consumed over 24 hours was determined (figure 10A). Insulin significantly increased the glucose consumed over 24 hours in de conditions with and without TNF-α. A change in insulin sensitivity (represented by the ratio of glucose consumed with and without insulin) is observed when TNF-α is added. The insulin sensitivity seemed to increase when TNF-α is added (figure 10B). So, TNF-α did not induce insulin resistance. However, TNF-α did have a significant effect on glucose consumption. Total amount of glucose consumed over 24 hours is decreased when TNF-α was added. So to conclude, TNF-α did not induce insulin resistance, however it did decrease total glucose consumption by the adipocytes.

Lactate production was increased by insulin and TNF-α

Lactate and pyruvate measurements were done to visualize the amount of pyruvate converted to lactate. In samples taken at the endpoint of the experiment lactate and pyruvate concentrations were measured. Lactate production was significantly increased when insulin or TNF-α were added (figure 11A). The concentration of pyruvate did not change significantly (figure 11B).

When the lactate production was compared with the glucose consumption we noticed the figures had a comparable pattern. When glucose consumption and lactate production of the both conditions without TNF-α were compared it was evident that lactate production did not exceed glucose consumption. However, in both conditions with TNF-α, lactate production exceeded glucose consumption. In the situation without insulin, glucose consumption was 0.6 mM and lactate production was 1.2 mM and in the situation with insulin, glucose consumption was 1.5 mM and lactate production was 1.8 mM. It is possible for lactate production to exceed glucose consumption, because one glucose molecule can be converted into two lactate molecules. At the start of the experiment we assume that there was no lactate present, since we used serum-free DMEM medium without lactate or pyruvate (with only L-Glutamine added). So, TNF-α increased the conversion of glucose to lactate.

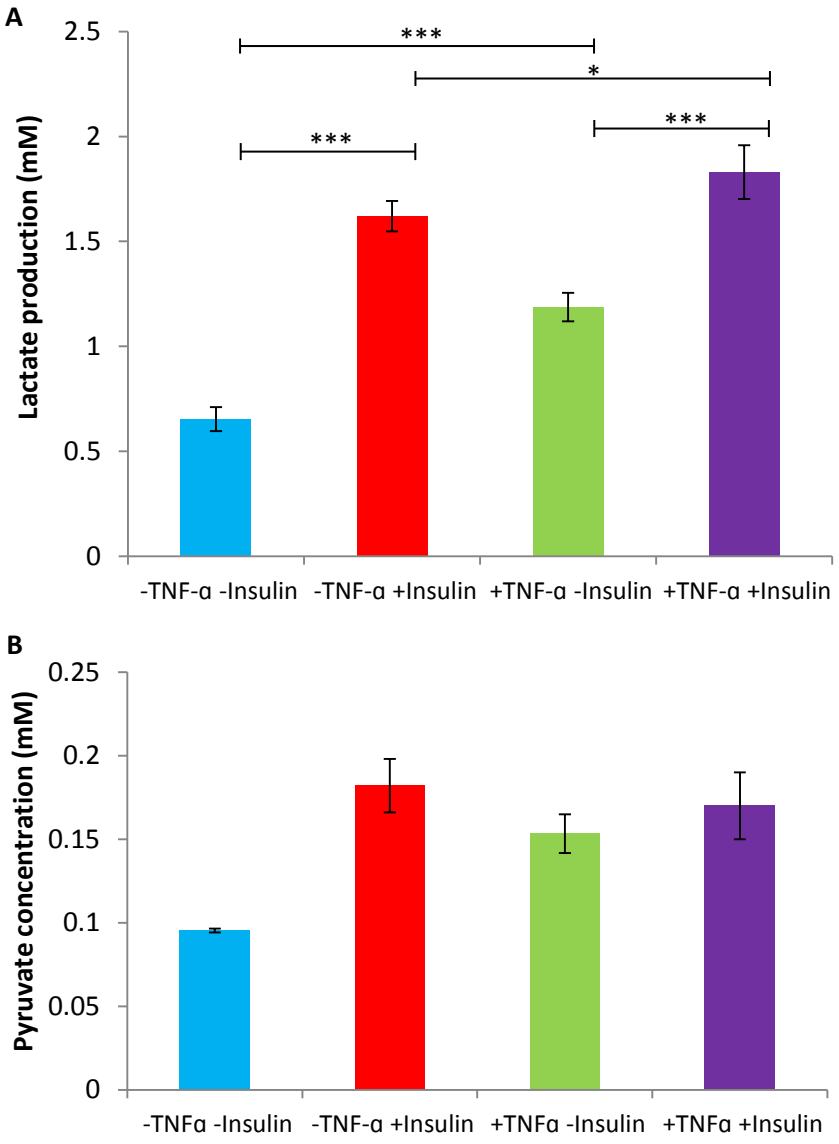

Figure 11. Effect of TNF-α and insulin on lactate production and pyruvate concentration. A) Lactate production. B) Pyruvate concentration. Blue: without TNF-α without insulin, Red: without TNF-α with insulin, Green: with TNF-α without insulin and Purple: with TNF-α with insulin. Error bars represent the standard deviation. * = $p < 0.05$ ** = $p < 0.01$ *** = $p < 0.001$.

Insulin increased activity of the glycolytic enzymes

To determine the effects of TNF-α and insulin on the enzyme activities, we did enzyme-activity assays. First it is important to note that the enzyme-activity assays of the 3T3L1 cells in the four conditions were only done once. Insulin increased the activity for most of the enzymes. The reason that not all enzymes respond the same to insulin is unknown at this moment. TNF-α did not have an effect on enzyme activities (Figure 12).

When the enzyme activity was compared with glucose consumption and lactate production, it became evident that for some enzymes the pattern was similar. The patterns were similar for the enzymes for which insulin seemed to have a stimulating effect on the activity.

To conclude, insulin had a stimulating effect on the activities of most enzymes and there was no detectable effect of TNF-α present.

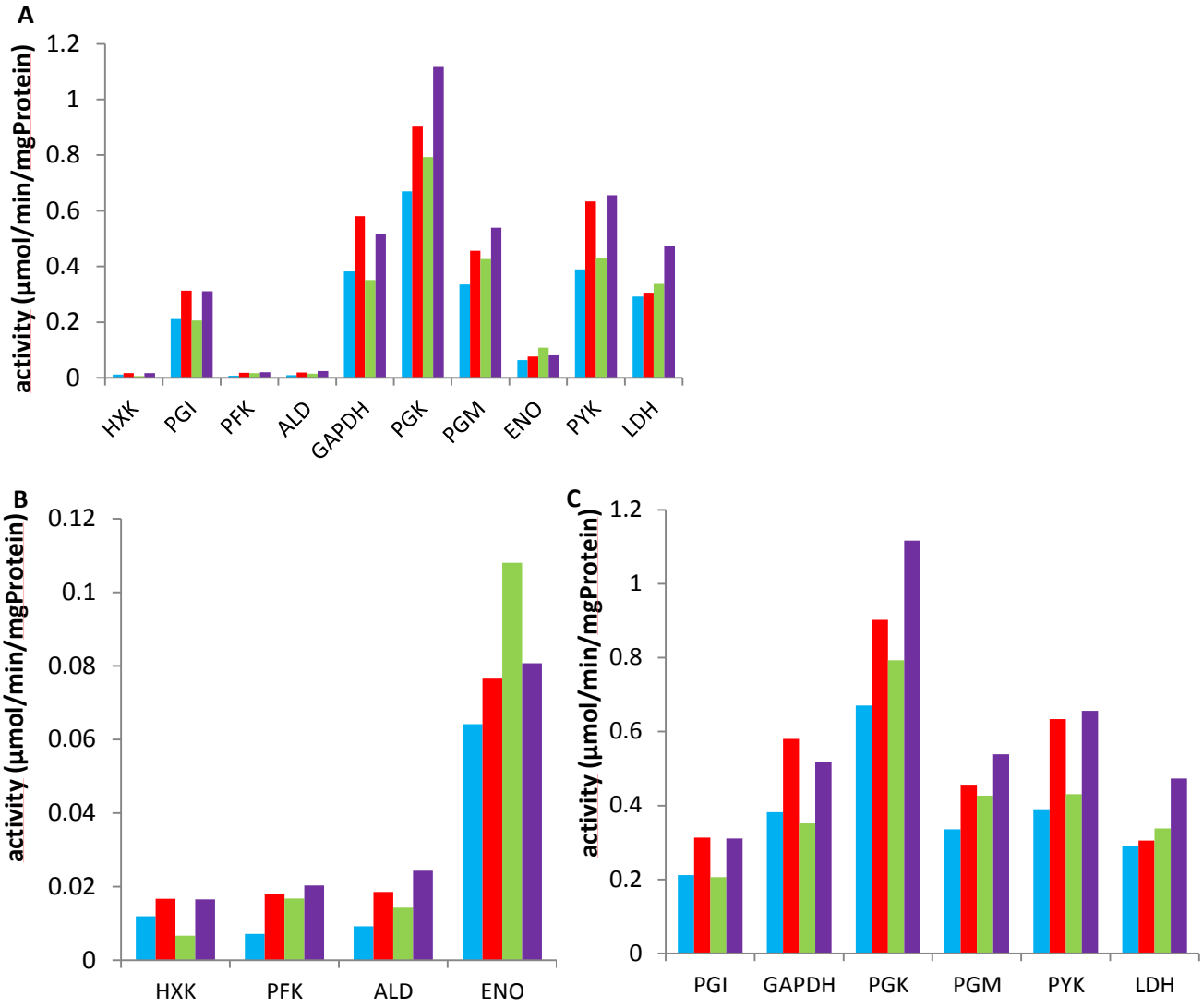

Figure 12. Effect of TNF-α and insulin on enzymatic activity. A) An overview of all enzymes. B) Enzymes with lower activity. C) Enzymes with higher activity. Blue: without TNF-α without insulin, Red: without TNF-α with insulin, Green: with TNF-α without insulin and Purple: with TNF-α with insulin.

DISCUSSION

In the current study we tried to induce insulin resistance in 3T3L1 cells by TNF-α to elucidate the effects of insulin on glucose metabolism. In previous studies it is shown that incubation of 3T3L1 cells with TNF-α induced insulin resistance in the glucose transport (Lo et al., 2013; Stephens & Pekala, 1991). Nevertheless, there are studies that used other methods to induce insulin resistance, for instance high levels of FFAs, dexamethasone and high insulin (Lo et al, 2013; She et al, 2014; Tan et al, 2015). One reason to choose TNF-α was that mice lacking TNF-α or the TNF-α receptor are protected to the development of insulin resistance (Hotamisligil, 2003). Which indicates that TNF-α really plays a role in insulin resistance. In our study, however, we did not observe insulin resistance based on the glucose consumption. TNF-α even seemed to increase insulin sensitivity in our glucose consumption experiment, while we tried to induce insulin resistance using a similar protocol as Lo et al., 2013 and Stephens & Pekala, 1991. However, our read out of insulin resistance was different, since we measured glucose consumption instead of glucose uptake. TNF-α could have different effects on these two mechanisms. At this moment, we cannot explain our deviating results.

But even though TNF-α did not induce insulin resistance, it did have some effects on the glucose metabolism. First, it decreased the glucose consumption of the cells. Second, it caused an increase in lactate production. These effects were observed when the cell conditions with and without stimulation of TNF-α were compared. The activity of the glycolytic enzymes was not changed by the addition of TNF-α. However, stimulation with insulin did have an effect. Insulin increased the activity for most of the enzymes. Moreover, insulin increased glucose consumption and lactate production.

Our results showed that the graphs of the enzyme-activities resemble the graphs of glucose consumption and lactate production. Enzymes in earlier stages of the glycolysis resemble the glucose consumption more, while the enzymes in later stages of the glycolysis resemble the lactate production more. HXK for example resembled the glucose consumption pattern and PGK resembled the lactate production pattern. The mechanism of insulin might influence the first glycolytic enzymes and the glucose consumption in the same way and also influence the later glycolytic enzymes and lactate production in the same way. And even though TNF-α had a lesser effect it probably also played a similar role in the resemblance of the patterns.

Insulin seemed to increase the activity of the GAPDH enzyme, while this GAPDH as often used as loading control assuming that its concentration is constant. The increased GAPDH activity could be explained in two ways. In previous studies it is shown that there is an insulin response element (IRE) in the upstream regulatory region of the GAPDH gene. It has been shown that IRE-A and IRE-B interact to enhance GAPDH transcription levels (Zhang et al., 2015). This suggests that insulin increases GAPDH expression by enhancing transcription (Zhang et al., 2015). This would mean that GAPDH is not a protein with such a constant concentration after all. However, a second option is that insulin can enhance phosphorylation of GAPDH by activation of Akt. If Akt phosphorylates GAPHD, the enzyme activity of GAPDH increases (Baba et al., 2010). This way it has no effect on the concentration, and could it still be constant. Since insulin might increase GAPDH concentration by increased expression, GAPDH should not be used as a loading control when insulin is used in the experiment.

Lactate production was increased by TNF-α. Pyruvate produced by the glycolysis can be converted either to acetyl CoA, after which it can enter the TCA cycle for oxidative phosphorylation or lactate by LDH (Phypers & Pierce, 2006). NADH is produced in the glycolytic pathway using NAD^+. NAD^+ can be regenerated in two ways, via oxidative phosphorylation or via the conversion of pyruvate to lactate (Berhane et al., 2015). If TNF-α negatively affects the oxidative phosphorylation, the conversion of

pyruvate to lactate could be increased to regenerate NAD^+. However, if this is the true mechanism behind the increase in lactate by TNF-α is unknown. Lactate is also increased in early stages of diabetes (Berhane et al., 2015), so the increase of lactate production when TNF-α is added could indicate a pre-stage of diabetes.

We used differentiated 3T3L1 cells for our experiments. We mentioned earlier in the result section, that the cells used in the second experiment were less differentiated. For this reason the results are not as reliable as the results of the first experiment. There are a few possibilities why fewer cells were differentiated. First, the cells were of lesser quality, since the cells grew evidently slower than the first batch of cells we differentiated. A second possibility is that during culturing we passed the cells once when the cell density was too high.
The protocol that we used for differentiation of the 3T3L1 cells was similar to other studies (She et al., 2014; Zebisch et al., 2012). The moment to start the differentiation and time frame of differentiation were alike and compounds used were mostly the same (She et al., 2014; Zebisch et al., 2012). Compared to the protocol of She et al. (2014) we even added a compound that increased the amount of differentiated cells, namely Rosiglitazone. The mechanism behind this probably is the activation of PPARγ, which helps overcome the differentiation block (Zebisch et al., 2012). With this information we can conclude our protocol for differentiation is appropriate.
To make sure future differentiations will be satisfactory, there are some recommendations we would like to make for the differentiation process. First, cells could be plated out in different densities. 48 hours after confluence cells are the most receptive to the differentiation compounds. When the cells are plated out in a few different cell densities there is a better chance that one of cell densities is in the best receptive state to start differentiation. Cells with the highest differentiation percentage can then be used for the experiments. The second recommendation concerns documentation. It would be good to document the amount of differentiated cells before the start of an experiment. Quantitative amounts of differentiated cells can be compared accurately between experiments using documentation. There are at least two ways to document the amount of differentiated cells. A picture could be taken of a few representative places of the wells. This can be compared between experiments. Another way to quantify is to count the differentiated cells. A way to do this is to choose a representative area of the well, for instance in the middle of the wells, and count the differentiated and the undifferentiated cells and determine the ratio. For best comparison it might be best to use both methods. In our opinion it is sufficient to document only once, just before you start the experiment.

Another point of discussion is what time frame to use for the experiment. In the first experiment a time frame of 24 hours was taken to measure glucose consumption, lactate production and changes in enzyme activity. However, changes took place only in the last 20 hours of the experiment, in which no measurement were done. For this reason we cannot make conclusions about the glucose-consumption rate. It might be that glucose consumption decreased steadily after the first four hours, or it could be that changes happened only after for example ten hours. We did a second experiment in which we tried to measure glucose consumption in a time frame of ten hours. Results are shown in supplement 2 figure 1, no detectable glucose consumption seems to be taking place over ten hours. However, these results are not reliable because of a lower amount of differentiated 3T3L1 cells. There are two possibilities: *i)* the results are correct, which means that there is a lag phase of glucose consumptions in the cells and the consumption of glucose starts after ten hours and *ii)* the glucose consumption happens within ten hours and the results of the second experiment are incorrect because the cells were not differentiated. To confirm one of the options, the experiment should be repeated. This has not been done because of insufficient time.

In other studies glucose consumption experiments were also done over a time frame of 24 hours (Li et al., 2007; Yin et al., 2002). However these studies were only interested in the endpoint of glucose consumption, to see the effects of different substances on glucose consumption. In literature we could not find other studies with a good time frame to determine the rate of glucose consumption.
During the experiments we also stimulated the cells with 100 nM of insulin. When cells are incubated with insulin for longer time, insulin resistance can be induced. In previous studies a decrease in insulin sensitivity was induced by 100 nM of insulin (for 24 or 48 hours) in 3T3L1 cells on glucose transport (Franekova et al., 2015; Lo et al., 2013). However, insulin sensitivity was less reduced than by TNF-α (Lo et al., 2013). Because insulin can induce insulin resistance over time, it is best to use a time frame as short as possible. But it is also important that changes in glucose concentrations are still detectable in time. Of course this all has an effect on the lactate production and enzyme activities as well. It is a possibility to stimulate glucose consumption with a lower concentration of insulin, for example 1 nM of insulin (Li et al., 2007), that way it will have less of an effect on inducing insulin resistance.
In the future we would like to harmonize our experiments with signalling experiments, to see what the mechanisms behind the changes are. The short time scale of signalling experiments must also be taken into account when searching for an optimal time frame.

In the experiments two concentrations of glucose were used, 1 mM and 5 mM. We continued with the concentration of 5 mM of glucose, because 1 mM was too low for the 24-hour experiment and because 5 mM is a physiological concentration (Kleman et al., 2009). Other studies also used about 5 mM of glucose in their glucose consumption experiments (Li et al., 2007; Yin et al., 2002). However, since we would like to measure in a shorter time frame in the future, it might be better to go back to a lower concentration of glucose, since otherwise the decrease in glucose concentration in the medium will not be large enough to detect.

Since there are still a few optimizations to make for the conditions of the experiment, it might better to switch to a cell type that does not have to be differentiated. This will save time of the differentiation, and decreases the chance that results are useless because of low quality differentiation. First optimize the conditions mentioned above, after that all cell types can be used.

To get to the stage where we can elucidate the complete glucose metabolism, a lot of research has to be done. When the conditions are optimal, enzyme assays can also be done under *in vivo* conditions and these results can be used to develop a quantitative computer model of the glucose metabolism. When a quantitative computer model is made, this can provide clarity about the effects of insulin on glucose metabolism. With this model predictions can be done about the effects of perturbations, like insulin resistance, on the glucose metabolism. This might help understanding the mechanisms behind insulin resistance and T2DM.

REFERENCES

Al-Goblan, A.S., Al-Alfi, M.A. & Khan, M.Z. 2014. Mechanism linking diabetes mellitus and obesity. Diabetes, Metabolic Syndrome and Obesity: Targets and Therapy. 7:587-591

American Diabetes Association. 2014. Diagnosis and Classification of Diabetes Mellitus. Diabetes Care. 37(Suppl. 1): S81-S90

Baba, T., Kobayashi, H., Kawasaki, H., Mineki, R., Naito, H. & Ohmori, D. 2010. Glyceraldehyde-3-phosphate dehydrogenase interacts with phosphorylated Akt resulting from increased blood glucose in rat cardiac muscle. FEBS Letters 584: 2796-2800

Barany, M (1996) Biochemistry of Smooth Muscle Contraction. New York: Academic Press

Bergmeyer. 1970. Methoden der enzymatischen Analyse herausgegeben von H.U. Verlag Chemie GmbH, Weinheim/Bergstr. Second edition

Berhane, F., Fite, A., Daboul, N., Al-Janabi, W., Msallaty, Z., Caruso, M., Lewis, M.K., Yi, Z., Diamond, M.P., Abou-Samra, A-B. & Seyoum, B. 2015. Plasma Lactate Levels Increase during Hyperinsulinemic Euglycemic Clamp and Oral Glucose Tolerance Test. Journal of Diabetes Research 2015, 7 pages

Boden, G. 2003. Effects of Free Fatty Acids (FFA) on Glucose metabolism: Significance for Insulin Resistance and Type 2 Diabetes. Experimental and Clinical Endocrinology & Diabetes 111: 121-124

Brietwieser, G.E., Altamirano, A.A. & Russell, J.M. 1990. Osmotic stimulation of Na+-K+-Cl- cotransport in squid giant axon is [Cl-]i dependent. American Journal of Physiology 258: C749-C753

Bruch, P., Schnackerz, K.D. & Grazy, R.W. 1976. Matrix-Bound Phosphoglucose Isomerase. Biochemistry 68: 152-158

Capursoa, C. & Capursob, A. 2012. From excess adiposity to insulin resistance: The role of free fatty acids. Vascular Pharmacology. 57: 91-97

Civelek, V.N, Hamiltont, J.A., Tornheim, K., Kelly, K.L., & Corkey, B.E. 1996. Intracellular pH in adipocytes: Effects of free fatty acid diffusion across the plasma membrane, lipolytic agonists, and insulin. Biochemistry 93: 10139-10144

Conley, K.E., Blei, M.L., Richards, T.L., Kushmerick, M.J. & Jubrias, S.A. 1997. Activation of glycolysis in human muscle in vivo. American Journal of Physiology 273: C306-C315

Feng, X.T., Wang, T.Z., Leng, J., Chen, Y., Liu, J.B., Lui, Y. & Wang, W.J. 2012. Palmitate Contributes to Insulin Resistance through Downregulation of the Src-Mediated Phosphorylation of Akt in C2C12 Myotubes. Bioscience Biotechnology Biochemistry. 76:1356-1361

Franekova, V., Angin, Y., Hoever, N.T.H., Coumans, W.A., Simons, P.J., Glatz, J.F.C., Luiken, J.J.F.P. & Larsen, T.S. 2015. Marine Omega-3 Fatty Acids Prevent Myocardial Insulin Resistance and Metabolic Remodeling as Induced Experimentally by High Insulin Exposure. Americal Journal of Physiology 308: C297-C307

Gibco (2001). Fetal Bovine Serum FAQs. Retrieved from: http://tools.lifetechnologies.com/content/sfs/brochures/B_08A00_0619_FBSInsert_bro.pdf on 15-06-15

Goldstein, B.J. 2002. Insulin Resistance as the Core Defect in Type 2 Diabetes Mellitus. The American Journal of Cardiology. 90: 3G-10G

Groen, A.K, Vervoorn, R.C, Van der Meer, R. & Tager, J.M. 1983. Control of gluconeogenesis in rat liver cells. The Journal of Biological Chemistry 258:14346-53

Guynn, R.W., Veloso, D., Lawson. R.J.W. & Veech, R.L. 1974. The Concentration and Control of Cytoplasmic Free Inorganic Pyrophosphate in Rat Liver in vivo. Biochemistry 140: 369-375
Hartstra, A.V., Bouter, K. E. C., Bächhed, F. & Nieuwdorp, M. 2015. Insight Into the Role of the Microbiome in Obesity and Type 2 Diabetes. Diabetes Care 38: 159-165

Hotamisligil, G.S. 2000. Molecular mechanisms of Insulin Resistance and the Role of the Adipocyte. International Journal of Obesity 24: S23-S27

Hotamisligil, G.S. 2003. Inflammatory pathways and insulin action. International Journal of Obesity 27:S53–55

Ingwall, J.S. 1982. Phosphorus nuclear magnetic resonance spectroscopy of cardiac and skeletal muscles. American Journal of Physiology 242: H729-H744

International Diabetes Federation (2014). Diabetes: Facts and Figures; IDF Diabetes Atlas, 6th edition update. Retrieved from http://www.idf.org/worlddiabetesday/toolkit/gp/facts-figures on 08-06-2015

Ishibashi, H. & Cottam, G.L. 1978. Glucagon-stimulated Phosphorylation of Pyruvate Kinase in Hepatocytes. The Journal of Biological Chemistry 253: 8767-8771

Janssen, L.J. & Sims, S.M. Acetylcholine activates non-selective cation and chloride conductances in canine and guinea-pig tracheal myocytes. Journal of Physiology 453: 197-218

Kahn, B.B. & Flier, J.S. 2000. Obesity and insulin resistance. The Journal of Clinical Investigation 106: 473-481.

Karalliedde, J. & Gnudi, L. 2014. Diabetes mellitus, a complex and heterogeneous disease, and the role of insulin resistance as a determinant of diabetic kidney disease. Nephrology Dialysis Transplantation. 0: 1-8

Kasuga, M. 2006. Insulin resistance and pancreatic β-cell failure. The Journal of Clinical Investigation. 116: 1756-1760

Kleman, A.M., Yuan, J.Y., Aja, S., Ronnett, G.V. & Landree, L.E. 2009. Physiological Glucose is Critical for Optimized Neuronal Viability and AMPK Responsiveness *In Vitro*. Journal of Neuroscience Methods 167: 292-301

Lai, M., Chandrasekera, P.C. & Barnard, N.D. 2014. You are what you eat, or are you? The challenges of translating high-fat-fed rodents to humand obesitiy and diabetes. Nutrition & Diabetes 4: 1-10.

Li, Y-Y., Wu, H-S., Tang, L., Feng, C-R., Yu, J-H., Li, Y., Yang, Y-S., Yang, B. & H, Q-J. The Potential Insulin Sensitizing and Glucose Lowering Effects of a Novel Indole Derivate *in vitro* and *in vivo*. 2007. Pharmacological Research 56: 335-343

Lidofsky, S.D., Xie, M.H., Sostman, A., Scharschmidt, B.F. & Fitz, J.G. 1993. Vasopressin Increases Cytosolic Sodium Concentration in Hepatocytes and Activates Calcium Influx through Cation-selective Channels. The Journal of Biological Chemistry 268: 14632-14636

Lo, A.K., Labadorf, A., Kennedy, N.J., Han, M.S., Yap, Y.S., Matthews, B., Xin, X., Sun, L., Davis, R.K., Lodish, H.F. & Fraenkel, E. 2013. Analysis of In Vitro Insulin-Resistance Models and Their Physiological Relevance to In Vivo Diet-Induced Adipose Insulin Resistance. Cell Reports 5: 259:270

De Luca, C. & Olefsky, J.M. 2009. Inflammation and Insulin Resistance. FEBS Letters 582: 97-105

Murphy, E., Steenbergen, C., Levy, L.A., Raju, B. & London, R.E. 1969. Cytosolic Free Magnesium Levels in Ischemic Rat Heart. The Journal of Biological Chemistry 264: 5622-5627

Oudard, S., Arvelo, F., Miccoli, L., Apiou, F., Dutrillaux, A.M., Poisson, M., Dutrillaux, B. & Poupon, M. F. 1996. High glycolysis in gliomas despite low hexokinase transcription and activity correlated to chromosome 10 loss. Britisch Journal of Cancer 74: 893-845

Østergaard, L.K. 1986. Associations between transport of alanine and cations across cell membrane in rat hepatocytes. American Journal of Physiology 251: G575-G584

Phypers, B. & Pierce, T.J.M. 2006. Lactate physiology in health and disease. Oxford Journals 6:128-132

Rorsman, P. & Trube, G. 1985. Glucose dependent K+-channels in pancreatic β-cells are regulated by intracellular ATP. Pflügers Archiv 405: 305-309

She, M., Hou, H., Wang, Z., Zhang, C., Laudon, M. & Yin, W. 2014. Melatonin rescues 3T3-L1 adipocytes from FFA-induced insulin resistance by inhibiting phosphorylation of IRS-1 on Ser307. Biochimie 103: 126-130

Stephens, J.M. & Pekala, P.H. 1991. Transcriptional Repression of the GLUT4 and C/EBP Genes in Adipocytes by Tumor Necrosis Factor-α. The Journal of Biological Chemistry 266: 21839-21845

Tan, S-X., Fisher-Wellman, K.H., Fazakerley, D.J., Ng, Y., Pant, H., Li, J., Meoli, C.C., Coster, A.C.F., Stöckli, J. & James, D.E. 2015. Selective Insulin Resistance in Adipocytes. The Journal of Biological Chemistry 250:11337-11348

Tschopp, J. & Schroder, K. 2010. NLRP3 inflammasome activation: the convergence of multiple signaling pathways on ROS production? Nature reviews 10: 210- 215

World Health organization (2015, January). Diabetes; Fact sheet N 312. Retrieved from http://www.who.int/mediacentre/factsheets/fs312/en/ on 05-06-2015

Yin, L., Hu, R., Chen, M., Tang, J., Li, F., Yang, Y. & Chen, J. Effects of Berberine on Glucose Metabolism in Vitro. Metabolism 51: 1439-1443

Zebisch, K., Voigt, V., Wabitsch, M. & Brandsch. 2012. Protocol for effective differentiation of 3T3-L1 cells to adipocytes. Analytical Biochemistry 425: 88-90

Zhang, J-Y., Zhang, F., Hong, C-Q., Giuliano, A.E., Cui, X-J., Zhang, G-J. & Cui, Y-K. 2015 Critical protein GAPDH and its regulatory mechanisms in cancer cells. Cancer Biology & Medicine 12: 10-22

SUPPLEMENTS

Supplement 1.

A

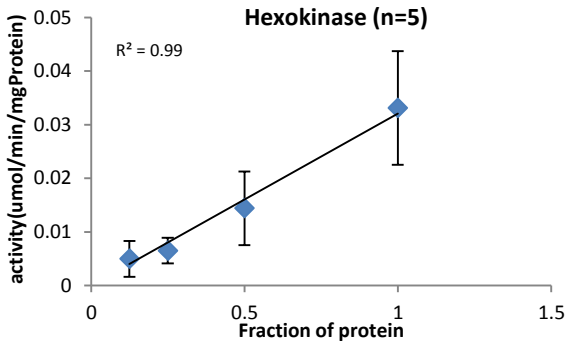

B

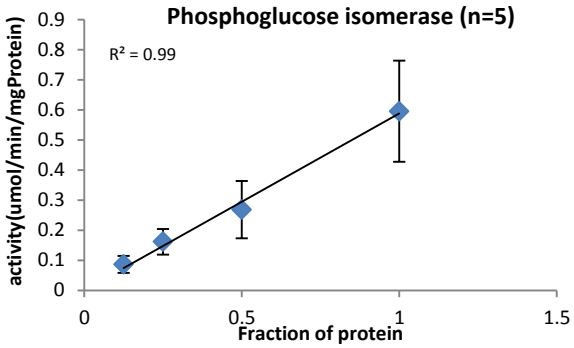

C

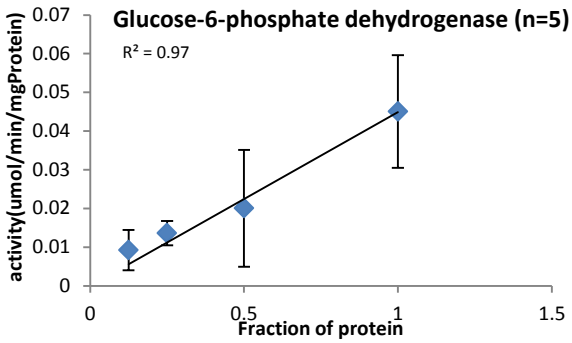

D

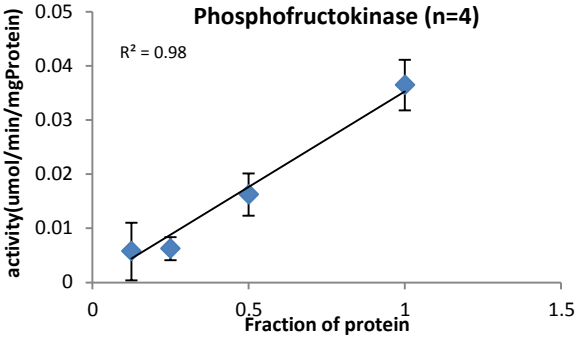

E

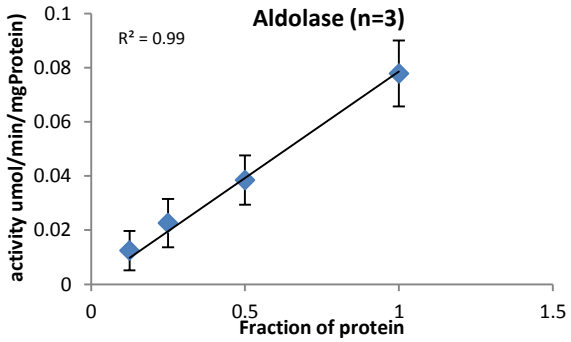

F

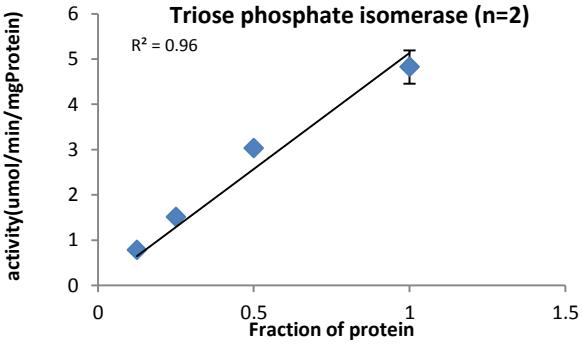

G

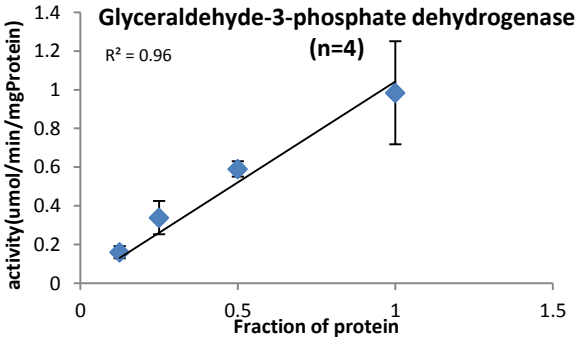

H

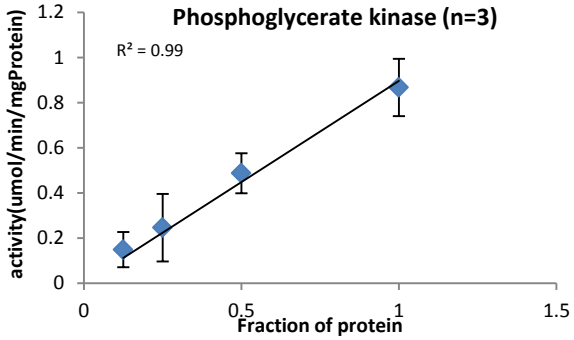

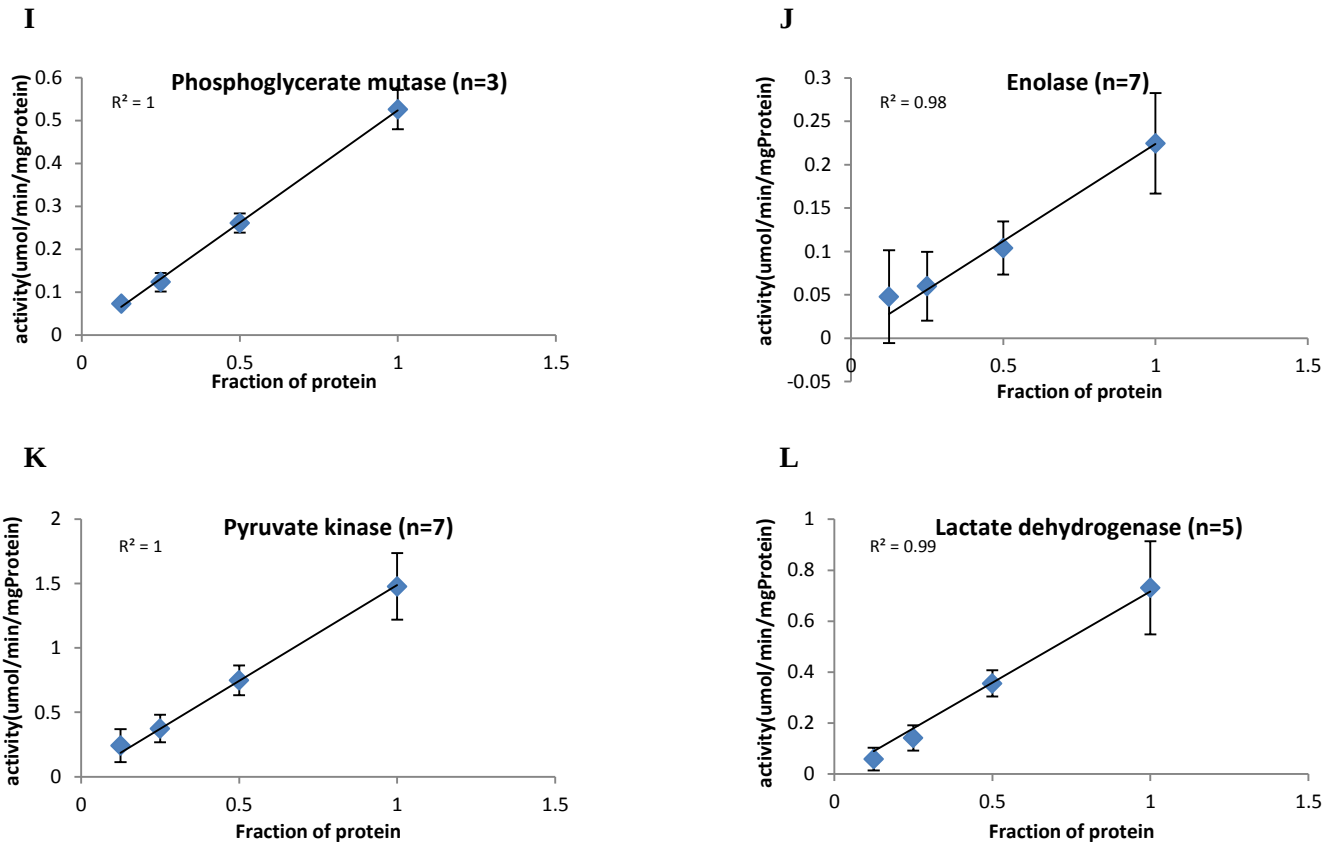

Supplement 1 figure 1. Average activity of the enzymes in dilutions in the in vitro medium. A) Hexokinase. B) Phosphoglucose isomerase. C) Glucose-6-phoshate dehydrogenase. D) Phosphofructokinase. E) Aldolase. F) Triose phosphate isomerase. G) Glyceraldehyde-3-phosphate dehydrogenase. H) Phosphoglycerate kinase. I) Phosphoglycerate mutase. J) Enolase. K) Pyruvate kinase. L) Lactate dehydrogenase. R^2 represents proportionality.

A

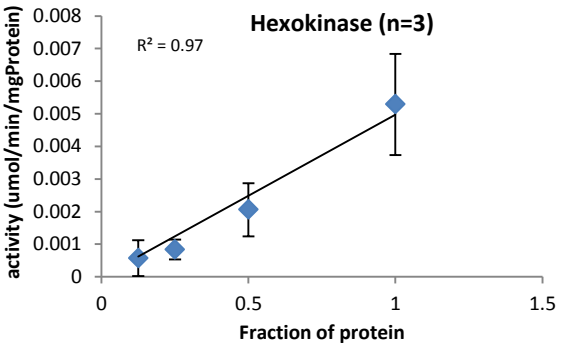
Hexokinase (n=3)
R² = 0.97
activity (umol/min/mgProtein)
0.008
0.007
0.006
0.005
0.004
0.003
0.002
0.001
0
0
0.5
1
1.5
Fraction of protein

B

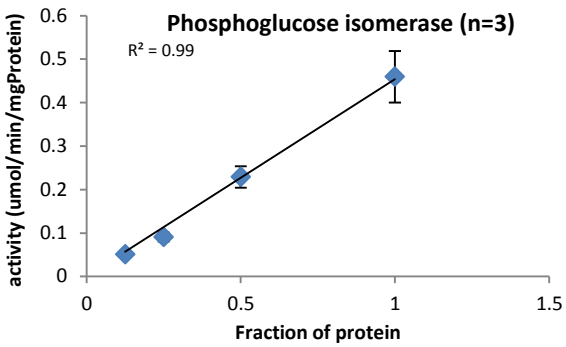
Phosphoglucose isomerase (n=3)
R² = 0.99
activity (umol/min/mgProtein)
0.6
0.5
0.4
0.3
0.2
0.1
0
0
0.5
1
1.5
Fraction of protein

C

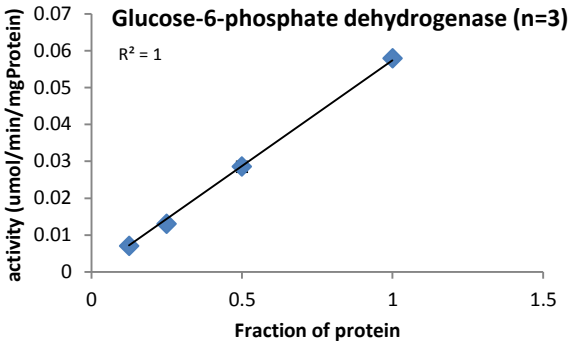
Glucose-6-phosphate dehydrogenase (n=3)
R² = 1
activity (umol/min/mgProtein)
0.07
0.06
0.05
0.04
0.03
0.02
0.01
0
0
0.5
1
1.5
Fraction of protein

D

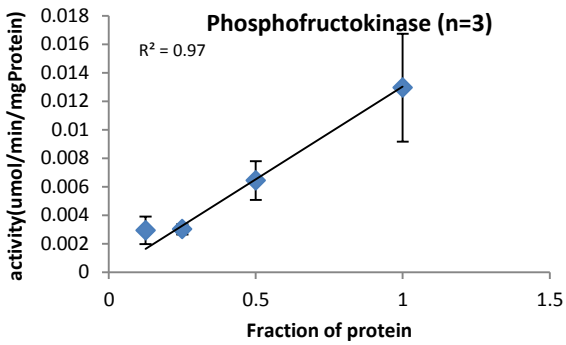
Phosphofructokinase (n=3)
R² = 0.97
activity(umol/min/mgProtein)
0.018
0.016
0.014
0.012
0.01
0.008
0.006
0.004
0.002
0
0
0.5
1
1.5
Fraction of protein

E

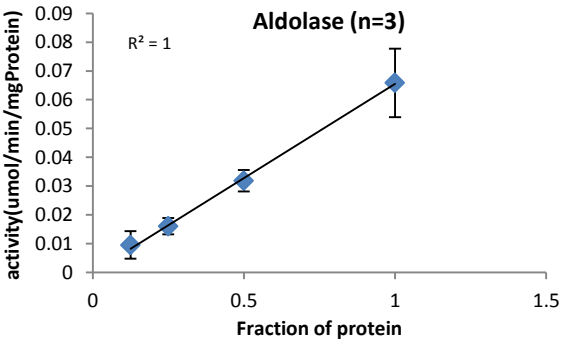
Aldolase (n=3)
R² = 1
activity(umol/min/mgProtein)
0.09
0.08
0.07
0.06
0.05
0.04
0.03
0.02
0.01
0
0
0.5
1
1.5
Fraction of protein

F

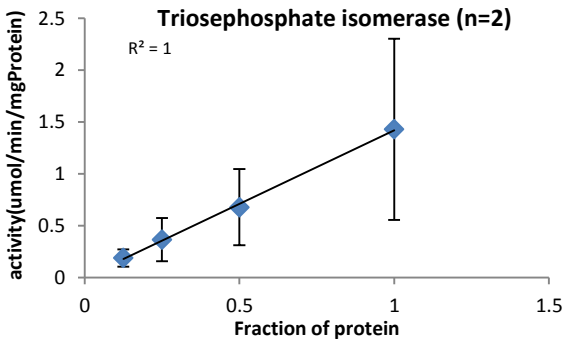
Triosephosphate isomerase (n=2)
R² = 1
activity(umol/min/mgProtein)
2.5
2
1.5
1
0.5
0
0
0.5
1
1.5
Fraction of protein

G

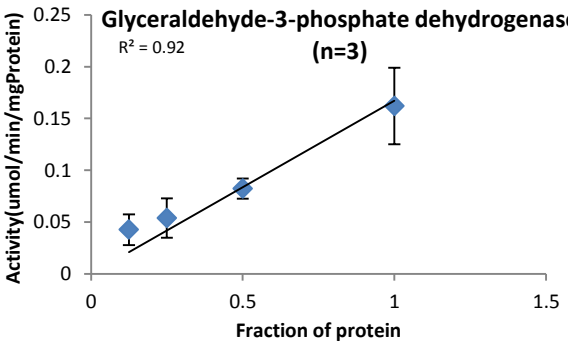
Glyceraldehyde-3-phosphate dehydrogenase (n=3)
R² = 0.92
Activity(umol/min/mgProtein)
0.25
0.2
0.15
0.1
0.05
0
0
0.5
1
1.5
Fraction of protein

H

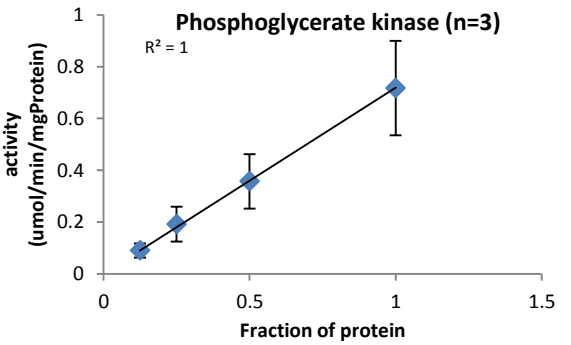
Phosphoglycerate kinase (n=3)
R² = 1
activity (umol/min/mgProtein)
1
0.8
0.6
0.4
0.2
0
0
0.5
1
1.5
Fraction of protein

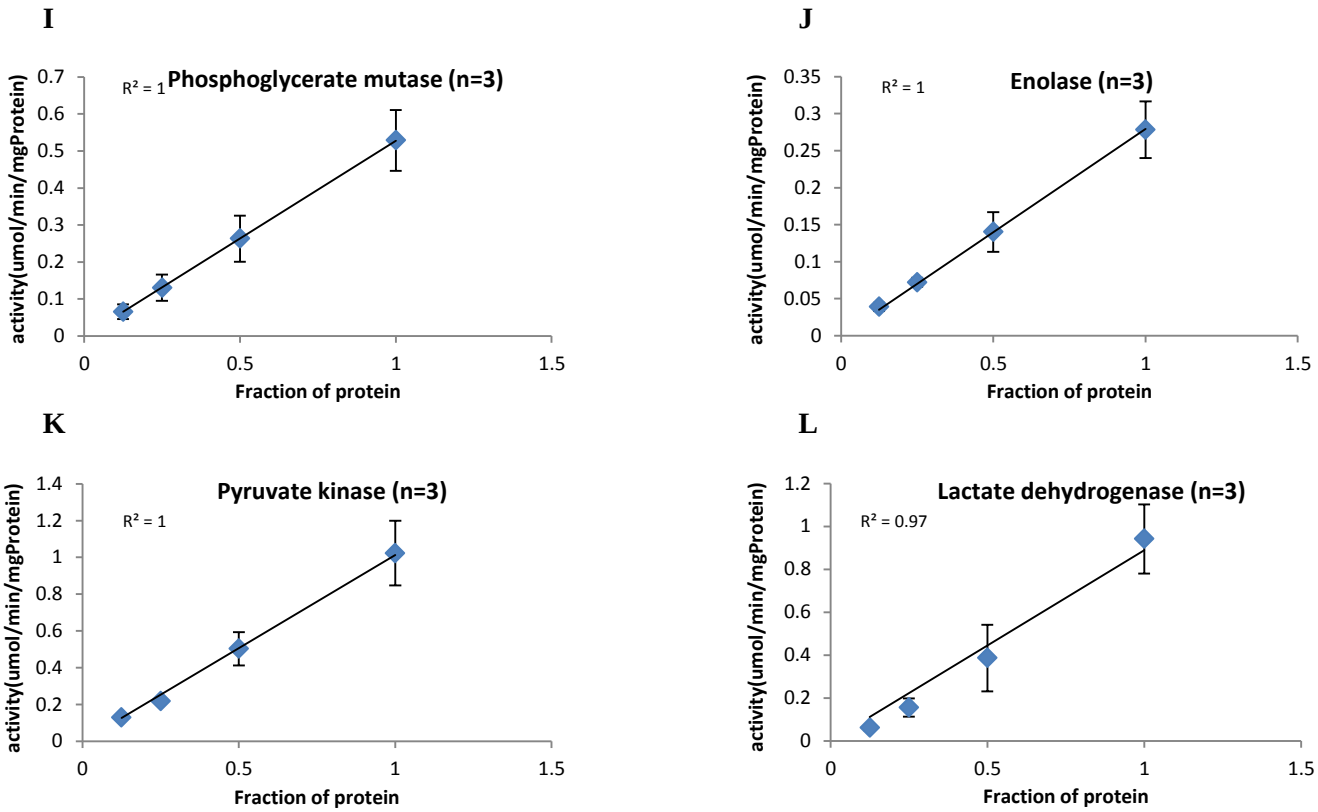

Supplement 1 figure 2. Average activity of the enzyme dilutions in the in vivo medium. A) Hexokinase. B) Phosphoglucose isomerase. C) Glucose-6-phoshate dehydrogenase. D) Phosphofructokinase. E) Aldolase. F) Triose phosphate isomerase. G) Glyceraldehyde-3-phosphate dehydrogenase. H) Phosphoglycerate kinase. I) Phosphoglycerate mutase. J) Enolase. K) Pyruvate kinase. L) Lactate dehydrogenase. R^2 represents proportionality.

Supplement 2.

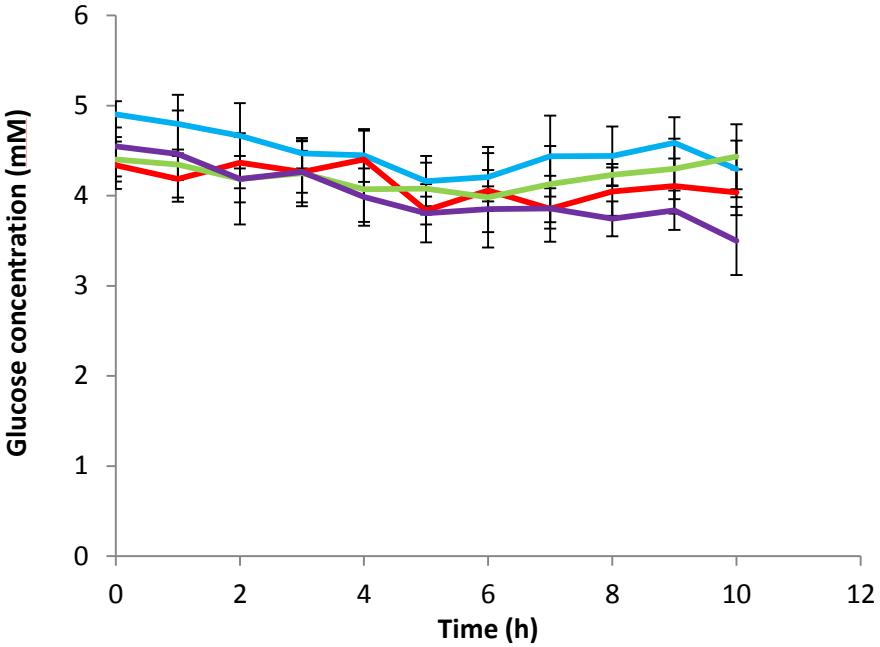

Supplement 2 Figure 1. Glucose consumption in 3T3L1 cells with a time frame of 10 hours. Blue: without TNF-α without insulin, Red: without TNF-α with insulin, Green: with TNF-α without insulin and Purple: with TNF-α with insulin.